RSC Advances

REVIEW

View Article Online
View Journal | View Issue

Cite this: *RSC Adv.*, 2026, **16**, 14259

Hydrogel-based delivery systems for cutaneous melanoma therapy: from chemical design and crosslinking strategies to structure–activity relationships

Yunying Wu,† Wei Zheng,† Xiao Li, Shengguang Wu, Liangliang Zhou, Ding Zhang* and Zhenhua Chen*

Cutaneous melanoma, a malignant neoplasm originating from melanocytes, has exhibited a steadily rising incidence worldwide. Conventional therapeutic strategies often suffer from limited precision, resulting in significant off-target toxicity or failure to prevent disease recurrence. Hydrogels have emerged as a promising platform for localized drug delivery in cutaneous melanoma treatment, owing to their chemically designable three-dimensional networks, tunable crosslinking strategies, and excellent biocompatibility. These structural features enable controlled, on-demand release kinetics and responsiveness to the tumour microenvironment, thereby facilitating multimodal therapy such as chemotherapy, radiotherapy, phototherapy, immunotherapy, and chemodynamic therapy, with enhanced therapeutic efficacy and reduced systemic toxicity. This review systematically examines the chemical composition and crosslinking strategies underpinning hydrogel design, with an emphasis on how these structural parameters influence therapeutic outcomes. Recent advances in tumour microenvironment-responsive hydrogels are further highlighted to elucidate the structure–activity relationships that inform the rational design of next-generation drug delivery systems.

Received 27th January 2026
Accepted 5th March 2026

DOI: 10.1039/d6ra00728g

rsc.li/rsc-advances

1. Introduction

Melanoma is a highly aggressive cutaneous malignancy arising from melanocytes, characterised by a high propensity for metastasis, therapeutic resistance, and poor clinical prognosis, and often referred to as the king of skin cancers. Over recent decades, the global burden of melanoma has intensified, with annual mortality rates showing a steady increase.[1] The primary cause of death in melanoma patients is visceral metastasis. Once tumour cells disseminate *via* hematogenous or lymphatic routes to vital organs, they proliferate and establish metastatic lesions that not only invade and disrupt normal organ architecture but also consume essential nutrients and impair physiological functions. Furthermore, widespread metastasis can

School of Pharmacy, Jiangxi Science & Technology Normal University, Nanchang 330013, Jiangxi, China. E-mail: zding888@126.com; zhenhuachen@jxstnu.edu.cn
† Co-first authors.

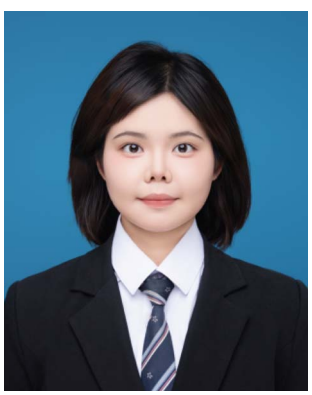

Yunying Wu

Yunying Wu is a graduate student in the School of Pharmacy at Jiangxi Science and Technology Normal University, under the supervision of Professor Zhenhua Chen. Her research focuses on the anti-melanoma effects of hydrogels.

Wei Zheng

Wei Zheng is a graduate student in the School of Pharmacy at Jiangxi Science and Technology Normal University. His current research focuses on the development of self-assembling nanomedicines for melanoma therapy.

induce systemic inflammatory responses, immune exhaustion, and cancer-associated cachexia, ultimately culminating in multi-organ failure or life-threatening complications. Lymph nodes are typically the first site of metastatic spread, while the lungs represent the most frequent location of distant metastasis. Although advances in immunotherapy and targeted therapy have significantly improved outcomes for patients with metastatic melanoma, a substantial proportion still experience disease progression despite treatment.[2,3] Particularly concerning is the elevated mortality observed among individuals aged 20–35 years. Geographically, Australia and New Zealand report the highest incidence rates globally, followed by Europe and North America.[4,5] While global age-standardised mortality rates and disability-adjusted life years have declined by 14.1% and 16.8% respectively, the mortality rate in certain regions, particularly Eastern Europe, continues to rise.[6]

Clinically, standard therapeutic approaches for melanoma encompass surgical resection, chemotherapy, and radiotherapy. In early-stage disease, complete surgical excision is often sufficient for effective disease control and is associated with favourable survival outcomes. However, upon progression to advanced or metastatic stages, melanoma becomes significantly more difficult to treat, leading to a marked decline in patient survival rates.[7,8] In recent years, the emergence of immunotherapy, hyperthermia, photothermal therapy (PTT), and photodynamic therapy (PDT) has significantly broadened the therapeutic landscape for cancer, driving a paradigm shift from conventional monotherapies toward integrated, sequential treatment strategies. In 2018–2019, the European Medicines Agency approved nivolumab and pembrolizumab for the removal of melanoma, marking a revolution in melanoma treatment.[9] Despite the notable efficacy of immune checkpoint antibodies targeting programmed cell death protein-1/programmed death-ligand 1 (PD-1/PD-L1) and cytotoxic T-lymphocyte-associated protein 4 (CTLA-4), as well as photothermal or photodynamic approaches in melanoma treatment, their clinical translation remains hindered by challenges including limited drug accumulation at tumour sites, inadequate tissue penetration, and systemic toxicity.[10,11] To address these limitations, there is growing interest in developing advanced drug delivery systems (DDS) capable of targeted delivery, controlled release, and multimodal synergistic therapy. Among the various platforms explored, such as nanoparticles, liposomes, and polymer microspheres, hydrogels have emerged as particularly promising candidates. Owing to their high water content, three-dimensional (3D) porous architecture, and injectable nature, hydrogels serve not only as effective drug reservoirs but also as modulators of the tumour immune microenvironment, offering a novel platform for localised combination therapy in melanoma.[10,12]

Hydrogels are 3D cross-linked networks formed by one or more polymers through diverse crosslinking strategies, including physical entanglement, chemical covalent bonding, and dynamic reversible interactions. Their molecular frameworks contain abundant hydrophilic functional groups, such as –OH, –COOH, –$CONH_2$, –SO_3H, and –NH_2, which confer excellent water-absorption properties.[13,14] The cross-linked structure

Xiao Li

Li Xiao is a master's student in Pharmacy at Jiangxi Science and Technology Normal University. She has received academic scholarships and excelled in innovation and entrepreneurship competitions. Currently, under her supervisor's guidance, she focuses on hydrogel synthesis and application in tissue repair.

Ding Zhang

Dr Ding Zhang received her PhD degree in Pharmaceutical Engineering from Dalian University of Technology, and currently serves as a Lecturer at the School of Pharmacy, Jiangxi Science and Technology Normal University. Her research focuses on the design and development of transdermal/mucosal drug delivery systems and the construction of nano-targeted delivery systems for applications in melanoma, psoriasis, and other diseases. She has published multiple articles in SCI journals, and has participated in three National Natural Science Foundation of China projects and three provincial projects.

Zhenhua Chen

Prof. Zhenhua Chen is a male PhD holder and a master's supervisor. He was selected for the Jiangxi Provincial Outstanding Youth Fund and Jiangsu Provincial High-Level Innovation and Entrepreneurship Talent Program. His roles include committee member of the Chinese Medicine Preparation Branch of the China Association of Chinese Medicine, Deputy Director of the Pharmacy and Traditional Chinese Medicine Teaching Steering Committee of Jiangxi Province, and Executive Director of the Jiangxi Pharmaceutical Association. His main research focuses on novel drug delivery systems and quality evaluation.

prevents dissolution upon hydration while maintaining structural integrity. These materials can be fabricated *via* chemically tunable crosslinking mechanisms and exhibit soft, rubber-like mechanical properties that closely mimic the native extracellular matrix (ECM), rendering them highly biocompatible and ideal for drug delivery applications. The 3D network provides ample space for physical entrapment of therapeutics, while functional moieties on the polymer chains facilitate drug loading through hydrogen bonding, electrostatic interactions, and ionic associations.[15] Notably, the selection of polymer composition and crosslinking strategy directly dictates the network architecture, degradation kinetics, and drug release behaviour. This structure–function relationship forms the foundation for the rational design of hydrogel-based DDS. Based on the drug delivery route, hydrogels can be classified into injectable, microneedle, nano-based, sprayable, and other types. Hydrogel-based DDS can form high local drug concentration zones at tumour sites, enabling sustained and controlled local release. This significantly reduces systemic toxicity to normal tissues and maximally suppresses local tumour recurrence, offering a highly translatable strategy for achieving clinical cure in cancer therapy.[16–20]

Excitingly, a new generation of stimuli-responsive "smart" hydrogels is transforming drug delivery paradigms. These materials are chemically engineered to sense and react to specific conditions within the cutaneous melanoma (CM) microenvironment, such as mildly acidic pH, overexpressed enzymes, or elevated levels of molecules like glutathione (GSH). They also respond to external triggers, including light, heat, or magnetic fields. Upon activation, the hydrogels undergo reversible or irreversible structural changes, such as swelling, collapse, or degradation, enabling on-demand, site-specific drug release. This capacity for precise spatiotemporal control positions smart hydrogel-based delivery systems at the forefront of cancer research (Fig. 1). Understanding the structure–activity relationships that link chemical design to responsive behaviour and therapeutic performance is therefore critical for advancing this field. This review systematically summarises recent advances in hydrogel-mediated delivery strategies for CM, with emphasis on chemical design principles, crosslinking strategies, and the resulting structure–activity relationships that govern therapeutic outcomes. A discussion of key achievements and persistent technical challenges is presented, aiming to provide a comprehensive reference and guide future developments in this rapidly evolving field.

2. Epidemiological characteristics and clinical management challenges of CM

CM arising from dysregulated melanocytes in the epidermal basal layer is a particularly aggressive form of skin cancer (Fig. 2a). During embryonic development, these melanocytes migrate and settle in the skin, periocular regions, and other tissues throughout the body.[21] Although CM accounts for less than 5% of all skin cancer cases, it is associated with the highest metastatic potential and contributes to approximately 75% of skin cancer-related deaths.[22–24] Over the past decades, the

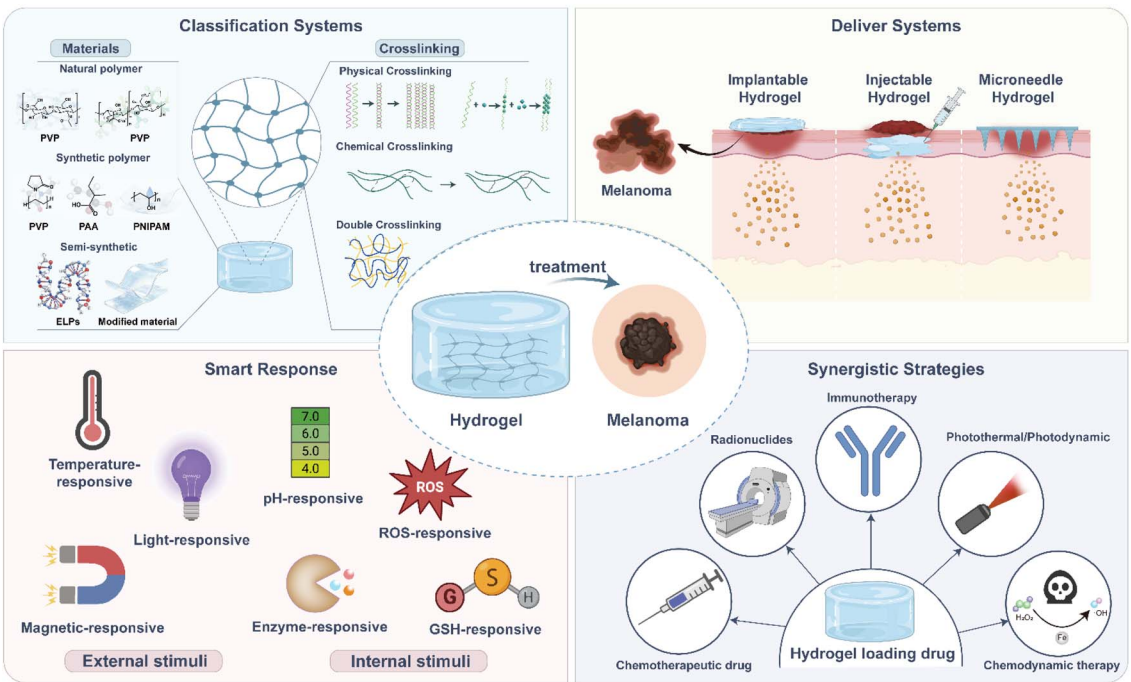

Fig. 1 Schematic illustration of a chemically designed hydrogel platform for cutaneous melanoma therapy. The composition, crosslinking strategy, and delivery geometry dictate the stimuli-responsive behaviour and drug release kinetics. Loading with diverse therapeutic agents (chemotherapeutics, radiosensitizers, immunomodulators, or agents for PDT/PTT/CDT) enables multimodal synergistic antitumor action.

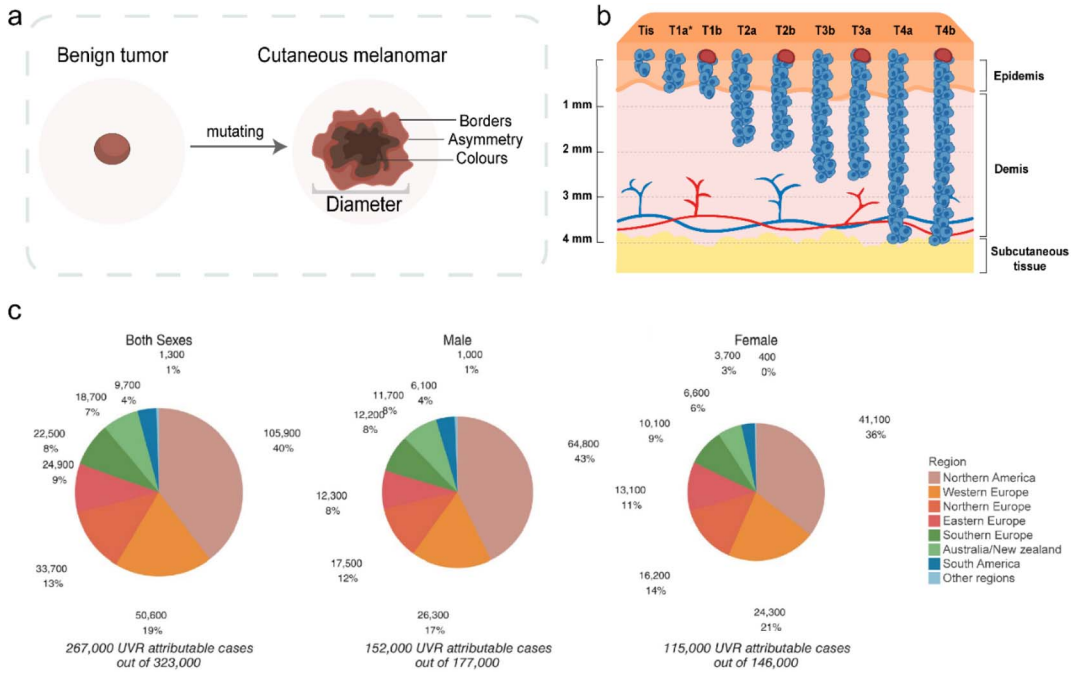

Fig. 2 (a) CM progression. (b) Progression and staging according to the eighth edition of the American Joint Committee on Cancer (AJCC). (c) CM attributable to UV radiation among people aged 30–99 by world region, 2022. Adapted with permission from ref. 31, Copyright 2025, Wiley-Liss.

incidence of CM has risen significantly and is projected to double within the next 20 years.[5] In clinical practice, according to the 8th edition of the American Joint Committee on Cancer (AJCC) TNM staging system (Fig. 2b), CM is classified into five main stages:[25,26] stage 0 (*in situ* melanoma), stage I (localized early disease), stage II (localized high-risk disease), stage III (regional lymph node metastasis or in-transit/satellite metastases), and stage IV (distant metastasis). The pathogenesis of CM is multifactorial, involving complex interactions between environmental exposures, genetic predispositions, and specific phenotypic traits such as fair skin and light hair colour.[27–29] Among these, ultraviolet radiation (UVR) represents the most significant environmental risk factor. This includes exposure from both natural sunlight and artificial sources. Chronic or repeated exposure to UVR induces cellular damage, ultimately leading to uncontrolled melanocyte proliferation.[30] As illustrated in Fig. 2c, approximately 80% of new CM cases among individuals aged over 30 worldwide were attributable to UVR in 2022, with similar attribution proportions between males and females. However, age-standardised data reveal a significantly higher burden of UVR-related CM in men compared to women.[31] Further research has found that mutational events in CM predominantly converge on two critical signalling pathways (Fig. 3). The RAS/RAF/MEK/ERK signalling pathway, also known as the mitogen-activated protein kinase (MAPK) pathway, represents the most frequently mutated target in CM. It drives aberrant cell proliferation by mediating oncogenic signal transmission. The phosphatidylinositol-3-kinase (PI3K)/AKT pathway, which regulates cell survival and resistance to apoptosis, represents the second major axis of dysregulation.[32]

In terms of treatment, wide local excision is the primary approach for early-stage CM. For patients with advanced disease, treatment relies on immunotherapies, such as anti-PD-1 antibodies, or targeted therapies for BRAF-mutant melanoma. Despite the significant survival benefit afforded by existing therapies, clinical management remains hindered by several critical bottlenecks. These include drug resistance, metastasis and recurrence, as well as limitations associated with conventional drug administration, namely poor targeting, severe toxic effects, and rapid drug degradation.

The unique physicochemical properties of hydrogels make them particularly suitable for local drug delivery applications. These properties enable precise and sustained drug release and local accumulation, thereby reducing systemic toxicity. Additionally, their aqueous preparation and dense network structure help to preserve the activity of therapeutic agents and improve the stability of biologics. By modulating their structural and release properties, hydrogels can act as drug reservoirs. This approach offers a new strategy for the local treatment of melanoma.

3. Classification and preparation of hydrogels

The properties and applications of hydrogels are fundamentally determined by both their compositional makeup and the manner in which their networks are formed. Hydrogels can be classified according to various criteria. Hydrogels can be broadly categorised by origin into natural, semi-synthetic, and synthetic types, each offering distinct biochemical and

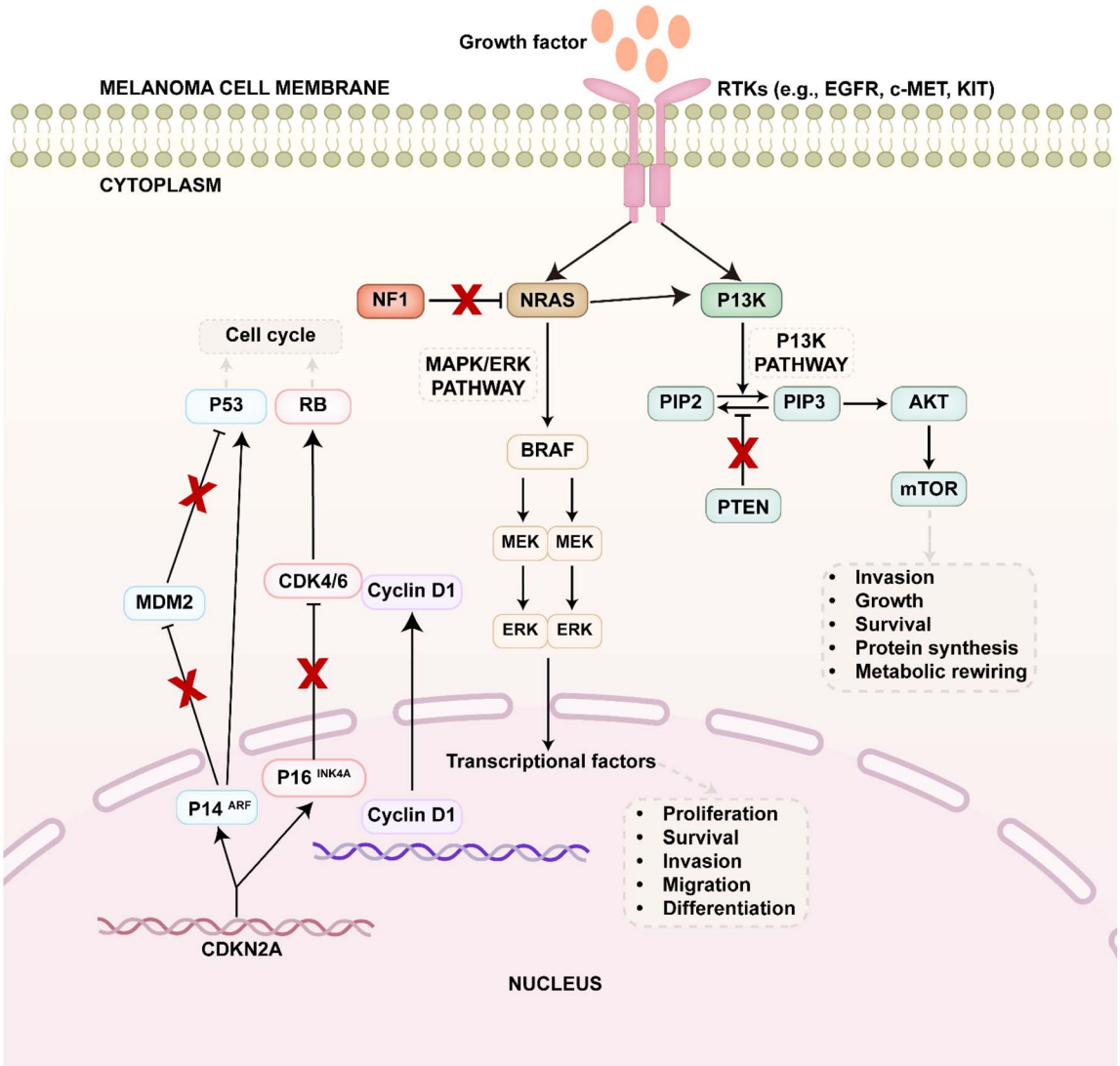

Fig. 3 Mutated driver genes and downstream signal pathways in melanoma.

mechanical characteristics. They can also be classified by their crosslinking mechanism into physical, chemical, or dual crosslinking categories, which govern network stability and responsiveness. The following sections provide an overview of hydrogel types based on their source materials, followed by a discussion of the various crosslinking strategies used in their preparation.

3.1. Classification of hydrogels

Hydrogels have attracted substantial interest in antitumor therapy. Such systems are characterised by a high water content, excellent biocompatibility, tunable structures, and favourable adaptability. As ideal carriers, they are used to introduce therapeutic agents into the body, and both treatment efficiency and safety are improved by controlling the rate, timing, and location of drug release. The origin of these hydrogels is therefore considered an important factor. As illustrated in Fig. 4, based on their sources, hydrogel materials are broadly classified into natural, synthetic, and semi-synthetic hydrogels.

3.1.1. Natural hydrogels. Natural hydrogels are formed through cross-linking of naturally occurring polymers. Among the various natural materials explored, the raw materials for natural hydrogels can be structurally classified into three categories: proteins and polypeptides (amino acid chains, such as collagen and elastin), polysaccharides (sugar chains, such as hyaluronic acid, chitosan, cellulose, and alginate), and nucleic acids (nucleotide chains, such as DNA and RNA). Based on their origin, these natural materials can be derived from plants, animals, or humans.

Natural polymer backbones contain abundant hydrophilic functional groups, such as hydroxyl, carboxyl, and amino groups. These groups can bind a significant number of water molecules, endowing the resulting hydrogels with high water absorption capacity and moisture content. This effectively mimics the hydrated environment of human tissues. Leveraging this structural advantage, desired gel matrices can be fabricated

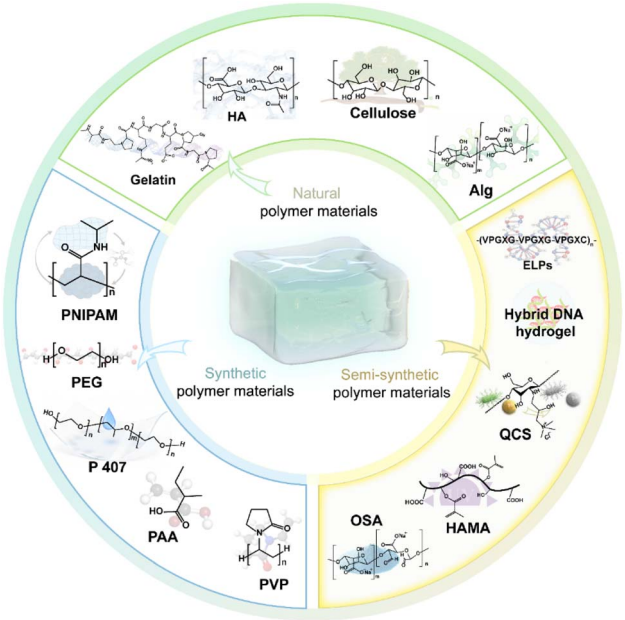

Fig. 4 Classification of hydrogels.

via physical or chemical cross-linking, using either single- or multi-component natural polymers. Furthermore, as these components are inherently derived from living organisms, they typically exhibit good biocompatibility, and their degradation products are non-toxic.[33] However, natural hydrogels also face significant limitations: poor mechanical strength, rapid and often unpredictable degradation rates, substantial batch-to-batch variability, high production costs, and potential risk of pathogen transmission associated with animal-derived variants.

Regarding natural hydrogel materials themselves, enzymatic degradation serves as the primary and specific breakdown pathway.[34] Within biological systems, enzymes such as matrix metalloproteinases, collagenases, hyaluronidases, and lysozymes can precisely recognise and cleave specific bonds (*e.g.*, peptide bonds and glycosidic linkages) within the hydrogel polymer chains. This enzymatic action decomposes the material into small molecular fragments, such as amino acids and monosaccharides, which are ultimately absorbed by cells or cleared from the body. In particular, when hydrogels are locally targeted to tumour sites, they exploit the unique tumour microenvironment. This microenvironment is often characterised by acidity and high enzymatic activity.[35] Acid-labile chemical linkages within the gel network, such as hydrazone or boronate ester bonds, become unstable under acidic conditions. Furthermore, hydrogels incorporating enzyme-specific peptide sequences can be recognised and cleaved by overexpressed enzymes, such as matrix metalloproteinase-2 (MMP-2), present in tumour tissue. Consequently, the hydrogel structure is disrupted specifically within the tumour microenvironment, leading to the controlled release of therapeutic agents. However, the tumour microenvironment is complex and heterogeneous.[36] A significant challenge arises because hydrogels composed solely of natural polymers (such as calcium alginate, gelatin, or hyaluronic acid),[33] which rely on simple ionic or amide bonds for cross-linking, often degrade too rapidly. This rapid breakdown hinders their ability to achieve long-term, sustained drug release. Consequently, there is a scarcity of advanced therapeutic research utilising such systems.

3.1.2. Synthetic hydrogels. Synthetic hydrogels are artificially engineered polymers fabricated through controlled chemical polymerisation techniques. They are particularly suitable when high demands are placed on material durability, mechanical strength, and water absorption capacity. Unlike natural hydrogels, synthetic variants allow precise tuning of stiffness, porosity, biodegradability, and biostability, making them ideal for engineered therapeutic platforms and reproducible manufacturing processes.[37,38] Specifically, commonly used synthetic hydrogel substrates include: poloxamer 407 (P407; also known as F127), poly(*N*-isopropylacrylamide) (PNIPAm), polyacrylic acid (PAA), poly(ethylene glycol) (PEG), *etc.*

Both P407 and PNIPAm are thermosensitive polymers. However, their mechanisms of gelation and drug release differ.[39] At low temperatures (4–10 °C), P407 remains in a liquid state, with micelles uniformly dispersed in solution. As the temperature rises, it undergoes a sol–gel transition. This shift is driven by enhanced hydrophobic interactions, which alter micellar morphology, promote aggregation, and intensify intermicellar forces, ultimately leading to gel formation. Drug release from P407 hydrogels typically occurs alongside gel degradation, enabling sustained and localised delivery. Owing to these properties, P407 is compatible with 3D printing extrusion and injectable systems, allowing *in situ* gelation following administration.[40] In contrast, PNIPAm hydrogels undergo a reversible volume phase transition from swelling to collapse at around 32 °C. This temperature is defined as the lower critical solution temperature (LCST) of PNIPAm hydrogels. The transition is driven by temperature-induced collapse and precipitation of polymer chains, which turns the solution turbid and eventually leads to gel formation. Based on this property, PNIPAm hydrogels can be loaded with photothermal agents such as polydopamine (PDA).[41] Upon light absorption, PDA converts light energy into heat. The resulting local heating triggers hydrogel contraction and facilitates drug release. This mechanism enables a temperature-controlled "on–off" release profile, allowing on-demand, repeated, and rapid pulsatile drug delivery.

In addition, PAA is a water-soluble anionic polymer synthesised *via* free radical polymerisation of acrylic acid monomers, featuring repeating units of $-[CH_2-C(=O)-C(OH)]_n-$, with pendant carboxyl groups (–COOH) whose ionisation state is pH-dependent.[42] The pH-sensitive nature of these PAA hydrogels permits targeted drug delivery in areas such as the gastrointestinal tract or tumour sites, improving treatment outcomes.[43]

PEG is a non-immunogenic polymer approved by the US FDA.[44] It exhibits excellent chemical inertness, hydrophilicity, and biocompatibility. PEG provides a stable, predictable platform for drug release and is widely employed in DDS, particularly for the development of sustained- and controlled-release

formulations. Its release kinetics are primarily governed by drug diffusion and network degradation, with low batch-to-batch variability.[45] This characteristic is especially critical for long-acting formulations that require consistent plasma drug concentrations, such as those used in hormone and protein therapeutics. Pure PEG hydrogels primarily rely on diffusion for small-molecule drugs or on bulk or surface erosion for macromolecular drugs.[46]

Unlike natural materials, which frequently exhibit batch-to-batch variability due to biological sourcing, synthetic hydrogels demonstrate high reproducibility and consistent performance across different production batches. This uniformity is critical for successful clinical translation, regulatory approval (*e.g.*, by the FDA), and large-scale industrial manufacturing.[47] Furthermore, their mechanical properties and chemical stability are highly tunable, with physicochemical characteristics precisely adjustable through controlled variation of monomer-to-crosslinker ratios.[48,49] However, synthetic hydrogels exhibit notable limitations. Their biocompatibility is often suboptimal, necessitating modification for optimisation. Furthermore, these materials generally degrade more slowly than their natural counterparts.

3.1.3. Semi-synthetic hydrogels. When the simultaneous tailoring of physical properties and efficient biological integration is required, hydrogels derived solely from natural or synthetic materials often have limited applicability. Semi-synthetic hydrogels have been developed to address this need. Their primary design objective is to retain excellent biocompatibility while enabling flexible modulation of chemical and mechanical characteristics.[50–52] For example, natural DNA can serve as a structural scaffold. Through rolling-circle amplification, artificially designed functional sequences, such as aptamers, CpG motifs, and restriction sites, are integrated into the scaffold.[53] This process yields a material with multiple tumour-responsive and therapeutic properties. The approach retains the innate biocompatibility of natural DNA while fully leveraging its programmability and sequence specificity. It therefore highlights the central strength of semi-synthetic materials, namely the fusion of a natural backbone with engineered functionality. The resulting hybridised DNA segments self-assemble into a 3D network through base pair complementarity and physical entanglement. Subsequent *in situ* encapsulation of enzyme-responsive nanoparticles within this network produces an injectable hydrogel. *In vivo*, the system initiates a cascade of events involving enzymatic cleavage, DNA strand breaks, GSH activation, and T cell responses.[54] This multistep cascade enables precise synergistic therapy that combines photodynamic and immune effects.

Cellulose lacks environmental responsiveness, and the strong hydrogen bonding among its molecular chains results in inadequate mechanical strength, poorly controllable degradation behaviour, and limited processability. To overcome these limitations, chemical modification is commonly employed to introduce substituents such as carboxymethyl, hydroxypropyl and methoxy groups, yielding derivatives including carboxymethyl cellulose (CMC), hydroxypropyl methylcellulose (HPMC) and methylcellulose (MC).[55,56] These modifications disrupt the crystalline architecture of cellulose at the molecular level, endowing it with new functionalities such as water solubility, thermal gelation or ion responsiveness. They also create reactive sites for subsequent crosslinking or grafting, enabling deliberate control over mechanical properties and degradation kinetics. For instance, CMC can form *in situ* physical gels *via* crosslinking between carboxyl groups and multivalent metal ions.[57] An increase in crosslinking density substantially improves the mechanical strength of the resulting hydrogel. The extent of crosslinking is governed by ion concentration, which in turn influences degradation time by modulating network porosity. Meanwhile, MC and HPMC undergo sol–gel transition at body temperature, rendering them suitable for injectable delivery systems.

Other commonly used semi-synthetic hydrogels encompass a diverse range. Representative examples include elastin-like polypeptide hydrogels and chemically modified polysaccharide-based hydrogels. Elastin-like polypeptides are a class of recombinant polypeptides inspired by natural elastin. Their repetitive pentapeptide sequence, valine-proline-glycine-Xaa-glycine (VPGXG), confers outstanding elasticity and thermoresponsiveness to the material.[58,59] By applying various crosslinking strategies, these peptides can be engineered into hydrogels with tunable mechanical properties and responsive behaviour. The introduction of additional click-chemistry functional groups, including azide and alkyne groups, enables orthogonal reactions to form irreversible covalent bonds. This provides precise control over viscoelastic properties.

Chemically modified polysaccharide-based hydrogels offer diverse functionalisation strategies. Through grafting or crosslinking, these modifications enable precise control over mechanical strength and degradation behaviour. Take methacryloylation as an example. Natural polysaccharides with reactive hydroxyl or amino groups can react with methacrylic anhydride. These include gelatin, hyaluronic acid, sodium alginate and chitosan.[60–63] When exposed to ultraviolet light, the modified polymers undergo free radical polymerisation. This process creates a stable and covalently crosslinked network. A higher crosslinking density improves both the compressive modulus and tensile properties of the hydrogel. At the same time, the denser network slows down enzymatic or hydrolytic degradation. This extends the material's degradation time both *in vitro* and *in vivo*.[64,65] Oxidative modification represents another common approach. In this process, polysaccharides are oxidised with sodium periodate or the TEMPO/NaOCl/NaBr system to generate aldehyde derivatives.[66–69] These derivatives undergo Schiff base reactions with amino-containing compounds, forming dynamic covalent bonds. This reversible crosslinking endows the resulting hydrogels with self-healing properties.[70] Although the mechanical strength of such networks is typically lower than that of irreversible covalent systems, it can be adjusted by varying the degree of oxidation or the concentration of crosslinker. In addition, the pH sensitivity of Schiff base bonds enables responsive degradation behaviour, with bond cleavage accelerated in acidic microenvironments. Furthermore, chemical derivatisation of chitosan offers a representative strategy for functional enhancement. The

introduction of carboxymethyl, quaternary ammonium, or thiol groups can substantially improve its water solubility, pH sensitivity and antibacterial activity. In particular, thiolated chitosan enables *in situ* crosslinking *via* intermolecular disulfide bonds, thereby enhancing the mechanical properties and mucoadhesion of the resulting gels. In contrast, incorporation of hydrophilic groups typically leads to faster degradation than that of unmodified chitosan.[71–74] In addition to methacryloylation, oxidation, and chitosan derivatisation, other modification approaches, such as esterification and sulphonation, have become key research directions in the field of polysaccharide-based hydrogels. The mechanisms by which these methods regulate mechanical and degradation properties are still being explored.

Throughout the trajectory of hydrogel development, natural hydrogels have established the foundation for biomedical applications owing to their excellent biocompatibility and low immunogenicity. However, their utility is constrained by insufficient mechanical strength and the difficulty of precisely controlling degradation behaviour. Synthetic hydrogels, by contrast, offer programmable control over mechanical properties, swelling behaviour, and degradation profiles through flexible molecular design. Yet they often lack cell recognition sites and active biological signalling. Semi-synthetic hydrogels have emerged in this context. Constructed with natural biopolymer backbones, they are chemically modified to introduce controlled crosslinking sites or functional groups. This approach retains the inherent advantages of biologically derived materials while enabling targeted enhancement of mechanical performance, degradation behaviour and responsiveness.

3.2. Preparation methods of hydrogels

Whether natural, synthetic or semi-synthetic, all hydrogels derive their 3D network structure and functional characteristics from the manner in which they are crosslinked. The crosslink density, the type of crosslink bonds, and the conditions that trigger crosslinking together shape the network's density and dynamics. These features, in turn, determine key material behaviours, including mechanical strength, degradation rate, swelling properties, and drug release. Depending on the crosslinking mode, hydrogels fall into three categories: physically crosslinked, chemically crosslinked, and dual crosslinked (Table 1).

3.2.1. Physical crosslinked hydrogels. The 3D network of physical hydrogels is not maintained by covalent bonds. Instead, it relies on the topological entanglement of polymer chains along with a range of physical interactions. These include electrostatic forces, hydrophobic interactions, hydrogen bonding, host–guest interactions, π–π stacking, and metal coordination.[75,76] Their formation mechanism involves spontaneous crosslinking of polymer segments *via* physical entanglements or reversible interactions, leading to macroscopic gelation. The dynamic reversibility of physical crosslinking points endows the system with stimuli-responsiveness, self-healing properties, and shear-thinning characteristics. These features directly govern the network's swelling behaviour, mechanical stability, and drug diffusion pathways. A key advantage of this approach is the absence of exogenous crosslinking agents and covalent bond formation, enabling fabrication under mild, biocompatible conditions.[77]

These dynamic, non-covalent bonds enable the formation of a 3D network within physically cross-linked hydrogels that is both environmentally responsive and adaptive.[78] The reversible nature of these bonds gives the network pores a distinct responsiveness and adaptability.[79] This characteristic positions these hydrogels as promising candidates for smart DDS, offering controlled release capabilities. However, this dynamism of the crosslinking points often results in relatively low structural stability and a broad pore-size distribution, creating challenges for precisely controlling drug-release behaviour.[80] In drug delivery applications, the pore size is a critical determinant of a drug's diffusion path and release kinetics:[81] larger pores facilitate the rapid release of macromolecular drugs, whereas a denser network can slow drug diffusion, enabling sustained long-term release.[82]

3.2.2. Chemical crosslinked hydrogels. Unlike physical hydrogels, chemical hydrogels achieve stable 3D networks through covalent crosslinking reactions.[83] Their construction relies on controllable chemical processes such as free-radical polymerisation, photo-induced crosslinking, Schiff base condensation, click chemistry, enzyme-mediated coupling, and Michael addition, all of which establish stable, irreversible covalent linkages that lock the network structure.[84,85]

Owing to the stable covalent linkages, chemically crosslinked hydrogels form a 3D framework with a fixed network structure.[86] This approach, which involves some dynamic covalent bonds that are reversible under specific conditions, endows the hydrogels with high mechanical strength and structural stability.[87,88] However, traditional irreversible crosslinking limits their ability to respond dynamically to external stimuli. Crosslinking density is a key factor in regulating the network structure. Specifically, a higher density leads to tighter binding between polymer chains, resulting in smaller pore sizes.[89] Under controlled crosslinking conditions, this distribution becomes more uniform, which in turn limits the penetration of macromolecular substances such as enzymes.[90] Conversely, increasing the proportion of crosslinking agents within an appropriate range raises the number of crosslinking points, strengthens the connections between molecules, and further enhances the overall stability of the network. In drug-release applications, this dense, stable network structure can effectively delay drug diffusion, making it particularly suitable for long-acting sustained-release systems.[80,91] However, the structural irreversibility and relatively fixed pore sizes associated with traditional crosslinking present challenges for regulation. The development of dynamic covalent chemistry is offering new pathways to overcome this limitation and achieve precisely controlled, stimuli-responsive release.[92]

Compared to physically crosslinked systems, chemically crosslinked hydrogels undergo sol–gel transition at lower polymer concentrations and exhibit superior mechanical properties: higher modulus, compressive strength, and shape

Table 1 Classification, definitions, and characteristics of hydrogel crosslinking methods[a]

Crosslinking method	Method	Definition	Properties	Ref.
Physical crosslinking	Hydrogen bonding	A directional and reversible interaction between a hydrogen atom and an electronegative atom	No chemical crosslinker needed (+) Low strength, brittle (−)	96 and 97
	Ionic bonding	Crosslinking is formed by electrostatic attraction between oppositely charged ions	Enhances conductivity, antibacterial properties (+) More brittle and softer, mechanical properties are affected by the environment (−)	97
	Hydrophobic interaction	When two or more nonpolar molecules are placed in a polar environment like water, hydrophobic regions aggregate, leading to structural interactions known as hydrophobic bonding	Good biocompatibility, high reversibility (+) Low mechanical strength (−)	98
	π–π stacking	Non-covalent interaction formed by overlapping π-electron clouds between aromatic rings	No chemical crosslinker needed, good reversibility (+) Low strength, poor stability (−)	99
	Salting out	High-concentration salt ions remove water molecules, causing hydrophobic regions of polymer chains to dehydrate and aggregate, forming a physical crosslinked network	Reversible tuning of mechanical strength, simple operation (+) Low strength, poor long-term stability (−)	98 and 100
	Electrostatic interaction	Attractive or repulsive interactions between charged groups, commonly used in polyelectrolyte hydrogels	Tunable swelling, responsive behaviour (+) Low strength, environmentally sensitive (−)	101
	Host–guest interaction	A process in which a "host" molecule forms an inclusion complex with a "guest" molecule	High reversibility, good responsiveness (+) Environmentally sensitive and mechanically weak (−)	75 and 101
	Metal coordination	Metal ions easily bind selectively and strongly to ligands, crosslinking polymer chains to form hydrogels	High strength, good responsiveness (+) Potential toxicity from metal ions (−)	102
Chemical crosslinking	Click chemistry	Hydrogels formed by reacting furan or furan derivatives with polyethene glycol dimaleimide	Low cytotoxicity, tunable mechanical properties (+) Performance may be unstable (−)	103
	Schiff base reaction	Formed by mixing aldehyde-functionalized and amine-functionalized biopolymers	Mild reaction conditions, wide applicability (+) Poor mechanical properties, low bioactivity (−)	104 and 105
	Photo-induced crosslinking	Crosslinking initiated by UV or visible light in the presence of a photoinitiator	Spatiotemporally controllable, suitable for bioprinting and *in situ* moulding (+) Requires additional initiator (−)	106
	Enzyme-catalysed crosslinking	Uses enzymatic reactions to form crosslinks between polymer chains	Efficient, highly selective, mild reaction conditions (+) Low mechanical strength, complex reaction conditions, enzyme stability hard to control (−)	77
	Michael addition	Nucleophiles containing thiol (–SH) or amino ($–NH_2$) groups react with α,β-unsaturated carbonyls *via* Michael addition to form covalent crosslinks	No additional crosslinker needed, controllable degradability (+) Potential side reactions (−)	99
	Amide bond	Covalent amide bonds are formed by the reaction between carboxylic acids and amine groups	High stability, good chemical strength (+) Harsh reaction conditions (−)	107
	Free radical polymerisation	Crosslinked networks formed by initiating monomer polymerisation with free radical initiators	Fast reaction, good controllability (+) Requires initiator, may leave residues (−)	105
Dual crosslinking		Simultaneous use of multiple physical crosslinking methods, such	High reversibility, good biocompatibility (+)	108 and 109

Table 1 (*Contd.*)

Crosslinking method	Method	Definition	Properties	Ref.
	Physical–physical crosslinking	as hydrogen bonding and hydrophobic interactions	Low strength (−)	
	Physical–chemical crosslinking	Introduction of both physical (*e.g.*, hydrogen bonding) and chemical (*e.g.*, Schiff base) crosslinking	Excellent overall performance, tunable mechanical strength (+) Complex preparation (−)	110 and 111
	Chemical–chemical crosslinking	Two different covalent crosslinking reactions (*e.g.*, click chemistry + free radical polymerisation) are carried out sequentially or simultaneously	Excellent mechanical performance, high stability (+) Complex process, risk of residual reagents (−)	105

[a] + And − respectively represent advantages and disadvantages.

fidelity, with degradation durations extendable from weeks to months.[93] These attributes make them ideal for long-term applications such as sustained protein delivery, 3D cell culture, and tissue engineering scaffolds. However, residual toxicants such as unreacted monomers, photoinitiators, catalysts, enzymes, or organic solvents may compromise drug stability, provoke inflammation, or damage surrounding tissues.[94,95] Therefore, when such reagents are used, rigorous post-processing (*e.g.*, dialysis, extraction) is required to reduce residuals below detectable levels, ensuring biosafety for *in vivo* use.

3.2.3. Dual crosslinked hydrogels. A single cross-linked network often fails to simultaneously fulfil the multiple therapeutic demands of mechanical support, dynamic responsiveness, and biological functionality. Researchers, therefore, commonly incorporate two or more cross-linking modes. Based on the types of mechanisms coupled, dual-crosslinked hydrogel can be grouped into three strategies: physical–physical, chemical–physical, and chemical–chemical.[112,113] In one study, Zhu *et al.*[109] covalently conjugated the indoleamine 2,3-dioxygenase 1 (IDO-1) inhibitor NLG919 with the β-sheet-forming peptide CGVVQQHKD *via* a disulfide bond. This process generated a peptide-drug amphiphilic prodrug, designated NLG-HKD. The NLG-HKD molecules self-assemble into nanofibres through β-sheet hydrogen bonding, which represents the first crosslinking event. These nanofibres subsequently organise into a 3D network *via* physical entanglement, constituting the second crosslinking. This strategy produces a physically crosslinked dual hydrogel that exhibits both shear-thinning and rapid self-healing. Similarly, Wu *et al.*[110] designed a physically dual-crosslinked nanocomposite hydrogel stabilised by cisplatin (CDDP)-peptide coordination bonds and electrostatic interactions between irinotecan-loaded alginate nanoparticles (IRlgNP) and peptides. Furthermore, the researchers integrated dynamic covalent bonds into the physically crosslinked network. This approach yielded a dual-crosslinked hydrogel that combines physical and chemical interactions. The material retains dynamic reversibility while achieving substantially enhanced mechanical stability. Fang *et al.*[111] developed a biomimetic, multifunctional, injectable hydrogel (CQCS@gel). The system's stability is achieved through a combination of interactions. It uses dynamic imine bonds formed between catechol-functionalized quaternized chitosan (CQCS) and dibenzaldehyde-terminated polyethene glycol (DB-PEG 2000) *via* a Schiff base reaction. The hydrogel is further stabilised within tissue by hydrogen bonding, ionic interactions, and covalent bonding from the catechol groups. Another study reported a chemically–chemically double-cross-linked bilayer hydrogel dressing that[105] constructed a chemically–chemically multi-cross-linked network by combining dynamic Schiff-base covalent bonds between oxidised hyaluronic acid (OHA) and CMCS with permanent covalent bonds generated *via* UV-initiated free-radical polymerisation of acrylamide. The resulting natural-polymer composite hydrogel exhibits outstanding antibacterial activity while simultaneously delivering high mechanical strength, fatigue resistance, and rapid self-healing.

Therefore, the precise selection of a single crosslinking strategy for specific medical scenarios, or the gradual integration of both physical and chemical crosslinking methods, could enhance the mechanical compatibility and biofunctionality of hydrogels. This approach may advance the clinical translation of hydrogel systems and improve their therapeutic efficacy.

It is noteworthy that different crosslinking strategies not only dictate the macroscopic properties of hydrogels, such as mechanical strength and degradation rate, but also fundamentally determine their core functionality as drug delivery systems. For instance, crosslinked networks based on dynamic covalent bonds, such as Schiff bases, can endow the system with self-healing capacity and stimuli-responsive release through the reversibility of the network. In contrast, networks formed by permanent covalent bonds are better suited for sustained drug release. Moreover, double-crosslinked hydrogels often exhibit more complex and diverse release behaviours, owing to their higher crosslink density and greater variety. Therefore, elucidating the structure–function relationship between crosslinking methods and delivery performance is essential for the rational design of hydrogel systems tailored for melanoma treatment.

4. Hydrogel-based delivery systems for CM therapy: modalities and release kinetics

Hydrogels for CM therapy can be categorised into distinct delivery modalities based on administration routes, including injectable hydrogels, microneedle-based hydrogels, nanohydrogels, and other topical formulations. Injectable hydrogels primarily target peritumoural tissues and postoperative defect sites. Leveraging their shear-thinning behaviour, these systems readily flow through needles during injection and undergo rapid *in situ* gelation at physiological temperature or in response to local microenvironmental cues. This enables the formation of a localised, long-acting drug depot at the tumour site or surgical cavity, facilitating sustained and controlled drug release.[114] Microneedle hydrogel patches are particularly suited for superficial melanoma lesions and postoperative adjuvant treatment. Fabricated with an array of micron-scale sharp projections, these patches efficiently penetrate the stratum corneum to create transient, uniform microchannels that significantly reduce skin barrier resistance. This enhances transdermal permeability while maintaining steady drug release kinetics, thereby improving therapeutic efficacy and patient compliance.[115] For patients with deep-seated or metastatic skin cancers, such as those involving arteries, veins, or muscles, nanohydrogels offer a promising therapeutic approach. Their high specific surface area and tunable surface chemistry enable efficient cross-barrier transport and active tumour targeting through ligand-mediated recognition. Notably, nano-hydrogels can co-deliver multiple therapeutic agents (*e.g.*, chemotherapeutics, immunomodulators) and imaging probes, supporting combinational therapy and real-time monitoring of treatment response.[116] Topical hydrogel formulations, such as sprays, gels, and adhesive patches, utilise the synergistic rheological properties of low shear viscosity for easy application and high zero-shear viscosity for prolonged residence. Topical hydrogel formulations, such as sprays and patches, utilise a combination of low-shear and zero-shear viscosities. This synergy facilitates easy spreading on the skin surface while ensuring prolonged adhesion. Consequently, these systems establish a localised high drug concentration within the skin layers, enabling sustained drug penetration and release.[117]

Beyond the diversity of administration routes, the therapeutic efficacy of hydrogel-based systems is critically governed by how therapeutic agents are loaded into the matrix and subsequently released. The loading capacity, spatial distribution of drugs within the hydrogel, and the kinetics of their release, which can range from burst release to sustained zero-order release or stimuli-triggered on-demand release, are fundamental parameters that determine local drug concentration, duration of action, and systemic side effects. These release behaviours are intricately influenced by the physicochemical properties of the hydrogel and the tumour microenvironment.[121] Therefore, rational design of loading strategies and precise modulation of release kinetics are essential to fully exploit the potential of each delivery modality. These aspects will be discussed in detail in Sections 4.5 and 4.6.

In summary, by rationally engineering the rheological behaviour, stimulus responsiveness, and biocompatibility of hydrogel carriers, precise and adaptable therapeutic strategies can be developed to address diverse clinical manifestations of CM.

4.1. Injectable hydrogels

Injectable hydrogels are typically formulated as low viscosity precursor solutions or preformed gels.[122] This design allows them to be delivered precisely to target tissues through minimally invasive injection. Their excellent injectability stems from their dynamic chemical networks. These systems are often constructed using dynamic covalent bonds, such as boronate esters and Schiff bases, or supramolecular interactions, including host-guest recognition, hydrogen bonds, and metal–ligand coordination.[123] These reversible crosslinking points endow the gel with shear-thinning behaviour. When the gel experiences high shear stress within a syringe needle, its dynamic crosslinked network rapidly dissociates. This dissociation causes a sharp drop in viscosity, allowing the material to flow smoothly. Once the injection is complete and the stress is relieved, the dynamic interactions quickly reform. The gel's viscosity recovers instantly, demonstrating self-healing properties. This physical responsiveness, driven by the dynamic reversibility of chemical bonds or intermolecular forces, ensures that the hydrogel can be delivered easily through a needle and promptly restore its structural integrity at the target site.

Upon deposition into a disease microenvironment, such as tumour tissues or post-surgical resection cavities, the system can utilise local physiological cues, including pH, temperature, specific ions, or reactive oxygen species (ROS) levels, to trigger a stimuli-responsive sol–gel transition.[124] The chemical basis of this transition lies in the enhanced physical entanglement, ionic coordination (such as the crosslinking of alginate with Ca^{2+}), or covalent crosslinking (through Schiff base reactions or enzymatic processes) among molecular chains in response to environmental changes.[125] This leads to the *in situ* formation of a stable 3D hydrogel network. With self-supporting mechanical integrity, this network can remain at the disease site for extended periods, thereby serving as a localised drug depot.

This ability to undergo *in situ* gelation at the tumour site or within the post-operative resection area positions injectable hydrogels as a highly promising platform for local drug delivery (Fig. 5a–c).[118] Compared to systemic administration routes like intravenous injection, this approach enables the establishment of a localised drug depot at the disease site, allowing high-dose co-delivery and sustained release of multiple therapeutic agents. By maintaining elevated local concentrations while minimising systemic exposure, injectable hydrogels effectively reduce peak plasma drug levels and mitigate off-target toxicity, thereby improving therapeutic safety and efficacy.[126]

Among these systems, injectable nanogels are colloidal suspensions composed of discrete hydrogel nanoparticles,

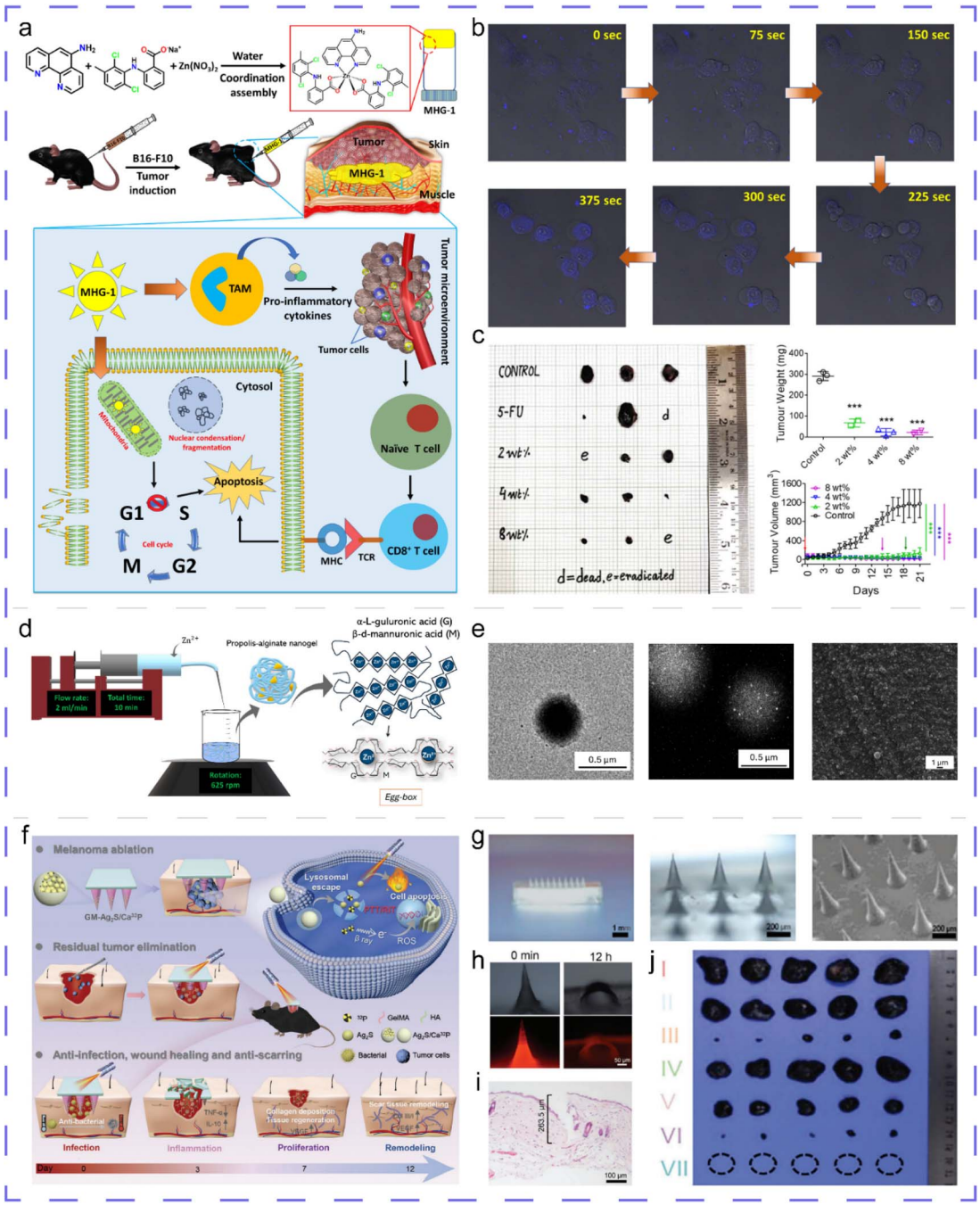

Fig. 5 (a) Schematic illustration of the self-assembled MHG-1 metallohydrogel synthesis and its PGE_2-downregulation-mediated chemo-immunotherapy for melanoma. (b) Internalisation of CC-1 (blue) triggers apoptosis. (c) Representative photographs and quantification of tumour volume (mm^3) and weight after 21-day MHG-1 treatment under the indicated conditions. Adapted with permission from ref. 118, Copyright 2023, Royal Society of Chemistry. (d) Schematic representation of propolis-loaded alginate/zinc nanogel (pNG) synthesis: alginate–propolis dispersion is combined in a beaker while Zn^{2+} solution is introduced *via* syringe pump for controlled mixing and gelation. (e) Illustrative TEM (bright- and dark-field) and SEM images of pNG. Adapted with permission from ref. 119, Copyright 2025, Elsevier. (f) Schematic illustrating the application of the GM-$Ag_2S/Ca_{32}P$ microneedle patch for treating postoperative melanoma recurrence and facilitating infectious wound healing. (g) Photograph, optical microscopy, and SEM images of GM-$Ag_2S/Ca_{32}P$. (h) Optical and fluorescence imaging of RhB-loaded GM-$Ag_2S/Ca_{32}P$ after microneedle insertion into mouse skin. (i) H&E staining of mouse skin after administration of the microneedle patch. (j) Photographs illustrating the gross tumour volume post-treatment across various groups. Adapted with permission from ref. 120, Copyright 2025, Wiley-VCH Verlag.

typically spherical, with diameters ranging from tens to several hundred nanometers.[127] Unlike the continuous, extending 3D polymeric network of macroscopic hydrogels, nanogels exist as discrete particles. They retain the advantageous properties of conventional hydrogels, including high water content, good biocompatibility, and tunable mechanical properties. Furthermore, their nanoscale dimensions impart unique properties, including a high specific surface area, small particle size, and an

enhanced ability to penetrate biological barriers (Fig. 5d and e).[119] Nanogel-based carriers support versatile administration routes, including intravenous, subcutaneous, and oral delivery, and have been widely explored for targeted transport of chemotherapeutics, nucleic acid therapeutics (*e.g.*, siRNA, miRNA), and immunomodulatory agents in skin melanoma therapy.[128–130]

4.2. Hydrogel microneedles

The stratum corneum presents a major physiological barrier to the transdermal delivery of numerous anti-tumour agents, severely limiting their cutaneous permeation and therapeutic efficacy.[131] To circumvent this challenge, microneedle (MN)-based transdermal delivery systems have been extensively developed, among which hydrogel microneedles (HMs) stand out as a particularly promising platform. HMs are made of highly hydrophilic polymer networks. Their penetration efficiency is closely related to the material's mechanical properties. Before skin insertion, HMs must possess sufficient mechanical strength and fracture toughness. These properties, which are determined mainly by crosslinking density and polymer composition, enable the needles to generate the axial stress needed to pierce the dense stratum corneum without buckling or fracturing.[132] Upon insertion into the skin, these microneedles rapidly uptake interstitial fluid; this action triggers the expansion of the matrix and dynamically alters the mechanical state of the microneedle tip. On one hand, the swelling process softens the microneedle through hydration. This allows it to conform to the skin's micromovements, reducing irritation. On the other hand, this volumetric expansion physically widens the microchannels further. Through this two-step mechanism, the process effectively disrupts the epidermal barrier. The first step relies on the initial strength for physical insertion. The subsequent step uses mechanical expansion stress to hold the channel open, triggering (Fig. 5f–j).[120] This coordination between the mechanical properties, which shift from rigidity to flexibility, and the physical structure enables the encapsulated therapeutic agents to bypass the dense stratum corneum barrier and be delivered efficiently into the dermis. The rate of drug release, although driven by mechanisms such as osmotic pressure and diffusion, is fundamentally governed by the evolution of porosity resulting from changes in crosslinking density. This factor is also a core parameter in the design of material mechanics. Therefore, by rationally adjusting the crosslinking density and polymer composition, it is possible to achieve both the high mechanical strength required for initial insertion and the adequate flexibility needed for subsequent swelling.[133] This balance enables efficient and painless transdermal delivery. Nevertheless, despite their advantages in minimally invasive administration and stimuli-responsive behaviour, HMs still face challenges related to limited mechanical robustness and susceptibility to premature degradation or deformation under storage or handling conditions, which may compromise their structural integrity and reproducibility in clinical applications.[134]

4.3. Implantable hydrogels

Postoperative recurrence and metastasis of melanoma primarily stem from residual microscopic disease and intraoperatively disseminated tumour cells that migrate *via* the vascular system and establish secondary lesions.[135] Although emerging nanotechnologies have improved drug accumulation in tumour regions, intravenously administered nanotherapeutics still suffer from limited overall bioavailability due to rapid clearance, off-target distribution, and poor tumour penetration. Due to the limited efficacy of systemic interventions such as chemotherapy and immunotherapy, the risk of tumour recurrence, proliferation, and distant metastasis remains a persistent clinical challenge. In response to these limitations, postoperative adjuvant strategies are increasingly shifting toward localised, long-acting DDS capable of maintaining therapeutic concentrations directly within the tumour resection bed. Implantable hydrogels, which can be applied *via in situ* injection or conformal coating onto tissue surfaces, offer a promising solution. Upon placement, they form a localised drug reservoir that enables sustained and gradient release over weeks to months. This prolonged pharmacokinetic profile allows for effective eradication of residual tumour cells while simultaneously sealing microcavities left after excision. Moreover, the 3D polymeric network of hydrogels acts as a physical barrier that restricts premature drug diffusion into systemic circulation, thereby minimising plasma exposure and reducing the risk of systemic toxicity.[136,137] As such, the application of drug-loaded implantable hydrogels to peritumoural tissues or surgical margins represents a rational and innovative strategy to suppress local recurrence and prevent distant metastasis following melanoma resection (Fig. 6a–d).[138]

4.4. Other types of hydrogels

Beyond the three conventional hydrogel delivery systems previously discussed, emerging formulations such as sprayable hydrogels, hydrogel suspensions, and thin-film hydrogels have recently gained attention as innovative approaches for treating superficial melanoma (Fig. 6e–i).[139–142] These platforms achieve directional drug release by immobilising micro- or nanospheres at the gel–tissue interface, thereby establishing a unidirectional diffusion barrier. This design ensures sustained therapeutic drug concentrations within the local microenvironment while restricting unintended penetration into deeper tissues, effectively minimising systemic exposure and associated toxicity. Upon application, these hydrogels tightly conform to the wound bed, forming an adherent, transparent film that enables real-time visualisation of wound-healing dynamics. Furthermore, their non-invasive nature allows for convenient replacement or supplemental dosing without disrupting the lesion site, significantly improving clinical manageability and treatment adaptability. Emerging hydrogel formats, such as sprayable and film-like types, remain in the preclinical validation stage. However, their distinct structural and functional advantages offer greater design flexibility for multimodal postoperative therapies. This potential is expected to accelerate the clinical translation of next-generation, flexible, and intelligent hydrogel fabrication technologies.

4.5. Strategies for therapeutic agent loading into hydrogels

Hydrogels offer multiple drug-loading mechanisms, including physical entrapment, covalent conjugation, nanocomposite

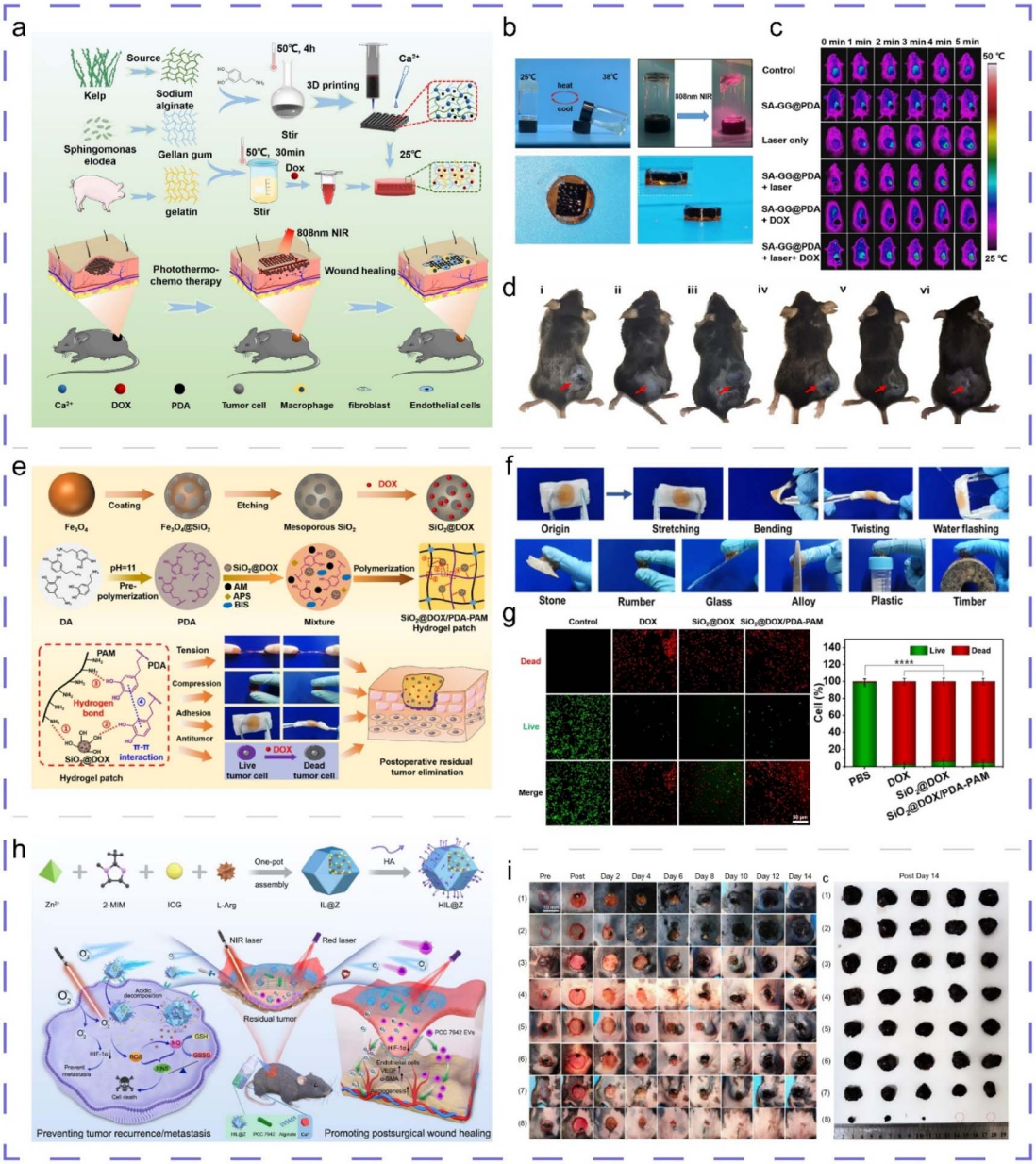

Fig. 6 (a) Schematic illustration of 3D printed heterogeneous SA-GG@PDA + DOX scaffolds for sequential tumour photothermal-chemotherapy and wound healing. (b) Photographs of the thermosensitive hydrogel undergoing phase transition upon heating (left) and 808 nm NIR irradiation (right), and front and side views of the resulting SA-GG@PDA + DOX heterogeneous scaffold. (c) The infrared thermal imaging of mice treated with different groups under an 808 nm (1.0 W cm^{-2}) laser for 5 min. (d) Photographs of mice from each treatment group. Adapted with permission from ref. 138, Copyright 2022, Royal Society of Chemistry. (e) Preparation of SiO_2@DOX/PDA-PAM Nanocomposite Hydrogel and the Application of Hydrogel in Antitumour Recurrence and Wound Healing after Local Tumour Surgery. (f) Adhesion properties of the SiO_2@DOX/PDA-PAM hydrogel. (g) Live/dead staining of B16 cells after 24 h treatment with SiO_2@DOX/PDA-PAM hydrogel. Adapted with permission from ref. 139, Copyright 2025, American Chemical Society. (h) Schematic illustration of sprayable HIL@Z/P/H for efficiently preventing tumour recurrence/metastasis and simultaneously promoting wound healing during the postsurgical cancer treatment. (i) Photographs of tumour/wound sites in different groups were taken over the 14-day treatment period, and the excised tumours were photographed on day 14 following different treatments. Adapted with permission from ref. 140, Copyright 2024, Springer Nature.

incorporation, and physical interactions.[143] This versatility enables the encapsulation of a diverse array of therapeutic molecules, ranging from small-molecule drugs to larger biomolecules such as proteins and nucleic acids.[144] Based on the distinct methods of drug-matrix binding, these mechanisms can be categorised into the following four types. Physical entrapment involves the direct incorporation of drugs into the hydrogel network, from which they are released *via* diffusion or material degradation. Kim *et al.*[145] developed a thermosensitive hydrogel based on Pluronic F127-grafted

gelatin, incorporating a temperature-sensitive F127-*g*-gelatin polymer network and loaded with both the BRAF inhibitor vemurafenib and an anti-PD-1 antibody for local chemo-immunotherapy of BRAF-mutant melanoma. In contrast to the passive loading of physical entrapment, covalent conjugation links drug molecules to the hydrogel backbone *via* chemical bonds, enabling more stable, controlled, and responsive release.[146] For instance, the previously mentioned NLG-HKD hydrogel is a covalently conjugated system in which the IDO-1 inhibitor NLG919 is attached to the peptide *via* a disulfide bond.[109] Beyond direct drug incorporation, researchers have developed more sophisticated delivery platforms, such as nanocomposite hydrogels. In this approach, a drug is first loaded into nanoparticles, like liposomes or polymeric micelles. These drug-loaded nanoparticles are then embedded within a hydrogel. This design enables multi-stage release kinetics and targeted delivery. Such nanocomposite systems are widely used.[147] A typical application involves encapsulating a hydrophobic drug within a carrier, which is subsequently integrated into the hydrogel matrix. For example, Chen *et al.*[148] fabricated a carboxymethyl chitosan-based hydrogel containing soybean lecithin–cholesterol nanoliposomes loaded with artesunate. This system was designed for dual-mode therapy of melanoma after surgical removal. In contrast to the carrier-based strategies described above, physical interactions offer a more direct and versatile approach for drug loading. These methods typically exploit the properties of the hydrogel network itself, using mechanisms such as electrostatic attraction, hydrogen bonding, or hydrophobic interactions to retain therapeutic agents.[149] Hydrogels designed for drug loading through physical interactions can be further divided into two categories. In the first step, drugs are loaded into a pre-formed hydrogel network by interacting with the polymer matrix. In the second, the drug molecules themselves act as gelators, self-assembling through intermolecular forces, including electrostatic or hydrophobic interactions, to form a carrier-free hydrogel. For instance, Su *et al.*[150] developed a fully physically cross-linked thermosensitive supramolecular hydrogel based on two-dimensional polydopamine nanosheets. This system was designed for combined photothermal and chemotherapy of melanoma. The hydrogel is constructed through a dual physical cross-linking mechanism. First, CPT-peg is loaded onto the surface of polydopamine nanosheets (PDAns) *via* π–π stacking and hydrophobic interactions, forming PDAns@CPT-peg. Subsequently, a second network forms through host–guest self-assembly and hydrogen bonding, in which α-cyclodextrin (α-CD) threads along the PEG chains to form inclusion complexes that aggregate into microcrystals. These two non-covalent interactions work synergistically, endowing the hydrogel with a high drug loading capacity, reversible gel–sol transition, injectability, and near-infrared (NIR) light-responsive drug release. Ding *et al.*[151] developed a carrier-free, injectable nanogel for chemoimmunotherapy in melanoma. The system relies on the co-assembly of thymopentin and doxorubicin (DOX) into a nanofibrous network. This design achieves a high drug loading capacity without additional carrier materials. It also enables responsive release tailored to the tumour microenvironment. The approach aims to augment the cancer-immunity cycle.

The mode of crosslinking between polymer chains within a hydrogel matrix bears a strong logical analogy to the incorporation of therapeutic agents into the gel. Among the four primary forms of drug loading, "physical encapsulation" involves simple entrapment, whereas "nanocomposite" loading entails the introduction of nanocarriers. Only "covalent binding" and "physical interaction" closely mirror the crosslinking mechanisms of "chemical crosslinking" and "physical crosslinking", respectively representing chemical bonding and non-covalent association between the drug and polymer chains.

4.6. Mechanisms of drug release from hydrogels

Once the loading strategy for a therapeutic agent has been determined, investigating its release kinetics from the hydrogel matrix is essential for optimising therapeutic outcomes. Release behaviour depends not only on the physicochemical properties of the drug but also on the hydrogel's network structure and degradation profile, as well as its responsiveness to external stimuli.[152] Based on the driving forces involved, drug release generally proceeds through mechanisms such as diffusion control, swelling or degradation control, and stimuli-responsive triggered release.[153]

Diffusion-controlled release is the most fundamental and commonly observed model, and it typically follows Fickian diffusion principles.[154] When the pore size of the hydrogel network exceeds the dimensions of the drug molecules and the polymer matrix remains structurally stable, the drug diffuses outward through the porous network driven by a concentration gradient. This process is primarily governed by the drug's molecular weight, hydrophobicity, and its physical interactions with the gel matrix. Drugs loaded through physical entrapment typically rely on this mechanism for release.[152] When the drug is incorporated *via* ionic complexation or hydrophobic interactions, the dissociation rate often becomes the rate-limiting step in the diffusion process.

The release of drugs controlled by swelling and degradation is primarily governed by the structural dynamics of the hydrogel matrix, rather than by simple molecular diffusion. For xerogels or preformed hydrogels with a low degree of swelling, exposure to a physiological environment triggers water penetration. This influx induces a transition of the polymer chains from a glassy to a rubbery state, enhancing their segmental mobility and expanding the network mesh size.[155] The resulting process constitutes swelling-controlled release. During this process, the drug gains sufficient space to diffuse outward. The release rate is closely related to the rate at which the swelling front moves forward. Typically, an initial lag phase, corresponding to the swelling process, is followed by a rapid release phase. The resulting release profile often conforms to swelling-mediated kinetic models, such as Schott's kinetic equation for swelling-controlled systems.[156] As a complementary mechanism to swelling, degradation-controlled release can be categorised into two distinct types.[157] The first is surface erosion, in which the hydrogel degrades layer by layer from the exterior inward. Here,

drug release occurs concomitant with the dissolution of the surface layers, and the release rate is directly proportional to the material's surface area. If a constant surface area is maintained, for instance in a cylindrical geometry, an approximately zero-order, constant release rate can be achieved. The second type is bulk degradation. In this case, water uniformly penetrates the entire gel matrix, and the degradation reaction takes place simultaneously throughout the whole volume of the material. As crosslinking points are cleaved or the polymer backbone is hydrolytically broken, the network structure gradually loosens. This allows the drug to diffuse out through the progressively enlarging pores. The release profile for bulk-degrading systems often exhibits an initial small burst, attributed to the diffusion of the drug located near the surface. This is followed by a period of slow release during the early stages of degradation. Subsequently, when the molecular weight of the polymer decreases to a critical threshold, a secondary release peak emerges, characterised by extensive matrix erosion and accelerated drug release. In the physically entrapped systems described above, drug release is primarily governed by diffusion in the initial phase, with degradation becoming the dominant mechanism in the later stages. By contrast, for hydrogels where the drug is covalently conjugated to the matrix, release is controlled exclusively by the kinetics of chemical bond cleavage.[157] For instance, drugs conjugated *via* ester linkages undergo hydrolysis by esterases or under alkaline conditions.[156] Those connected through disulfide bonds are cleaved in reducing environments with high GSH concentrations. In such cases, bond cleavage must occur before the drug can diffuse. Therefore, the degradation process, specifically bond breaking, becomes the rate-limiting step for the entire sequence.[158]

The final category, stimuli-responsive release, is associated with the smart properties of hydrogels, enabling on-demand drug delivery under specific pathological conditions or in response to external stimuli. This mechanism relies on switchable structures within the gel that respond to particular signals. Such a design improves therapeutic precision and efficiency, while also reducing systemic side effects. Stimuli-responsive release will be introduced in the following chapters.

In summary, the release of drugs from hydrogels is not a random process. It is precisely controlled by the material's chemical structure, including factors such as crosslinking density, pore size, and the nature of functional groups. This link between release kinetics and material structure represents a core aspect of the structure–activity relationship.

5. Application of smart responsive hydrogels in CM

Over the past five years, stimulus-responsive hydrogels, often called smart hydrogels, have attracted increasing research interest in the field of pharmaceutical sciences. They have now emerged as a prominent focus in modern pharmaceutics. These hydrogels can undergo reversible or irreversible structural transformations in response to external or internal stimuli such as temperature, pH, enzymes, light, and magnetic fields. Such stimuli-triggered changes are precisely reflected in dynamic alterations of mechanical strength, swelling behaviour, hydrophilicity, and permeability to bioactive molecules, enabling spatiotemporally controlled and on-demand release of anticancer agents.[159,160] The application of stimulus-responsive hydrogels in CM therapy not only enhances the therapeutic efficacy of encapsulated drugs but also minimizes off-target effects on healthy tissues, thereby offering a promising platform for precision medicine in oncology.[161]

5.1. pH-responsive hydrogels

The anaerobic glycolysis prevalent in tumour tissues results in a characteristically acidic TME, creating a distinct pH gradient between malignant and healthy tissues. The extracellular pH of tumours is typically around 6.5, while the intracellular pH can drop to approximately 5.0. In response to such microenvironmental changes, pH-sensitive hydrogels undergo a cooperative transformation in their network structure.[162] This change is typically driven by the protonation or deprotonation of functional groups, such as amino or carboxyl groups, on the polymer chains, or by the cleavage of dynamic chemical bonds, including Schiff bases or boronate esters, under acidic conditions.[163] These processes can result in hydrogel swelling, shrinking, or network degradation. Consequently, the drug release behaviour is correspondingly altered. In a neutral physiological environment, the hydrogel network remains tight, resulting in slow drug release that approximates zero-order kinetics. However, upon exposure to the acidic tumour microenvironment, the network structure loosens or disintegrates, thereby substantially accelerating drug release. This enables on-demand or triggered release specifically at the lesion site, effectively avoiding the systemic toxicity associated with conventional chemotherapy.[164,165]

Building on this mechanism, researchers have designed multiple pH-responsive hydrogels for combination tumour therapy. Yu *et al.*[166] developed a self-healing, pH-responsive hydrogel by crosslinking 3-carboxyphenylboronic acid-grafted chitosan (CS-BA) with PVA, incorporating tannic acid/iron nanocomposites (TAFe). This design leverages the dissociation of dynamic bonds under acidic conditions to achieve network restructuring. The incorporation of TAFe further endows the system with the ability for on-demand chemodynamic therapy, effectively preventing postoperative tumour recurrence both *in vitro* and *in vivo* (Fig. 7a–c). To accurately match the tumour pH gradient, Lin *et al.*[167] fabricated a novel injectable hydrogel delivery platform using chitin nanofibers and dialdehyde alginate as building blocks, crosslinked *via* dynamic Schiff base bonds. At pH 7.4, the system exhibited a stable structure and sustained release behaviour. However, under acidic conditions that mimic the tumour microenvironment at extracellular pH 6.5 and intracellular pH 5.5, network degradation accelerated. This change led to a faster release rate of the model drug DOX, demonstrating excellent microenvironment-responsive properties. Furthermore, Huang *et al.*[168] pushed the concept of on-demand release to the extreme, designed a pH-responsive dissolvable microneedle system (DHA@HPFe-MN) co-loaded

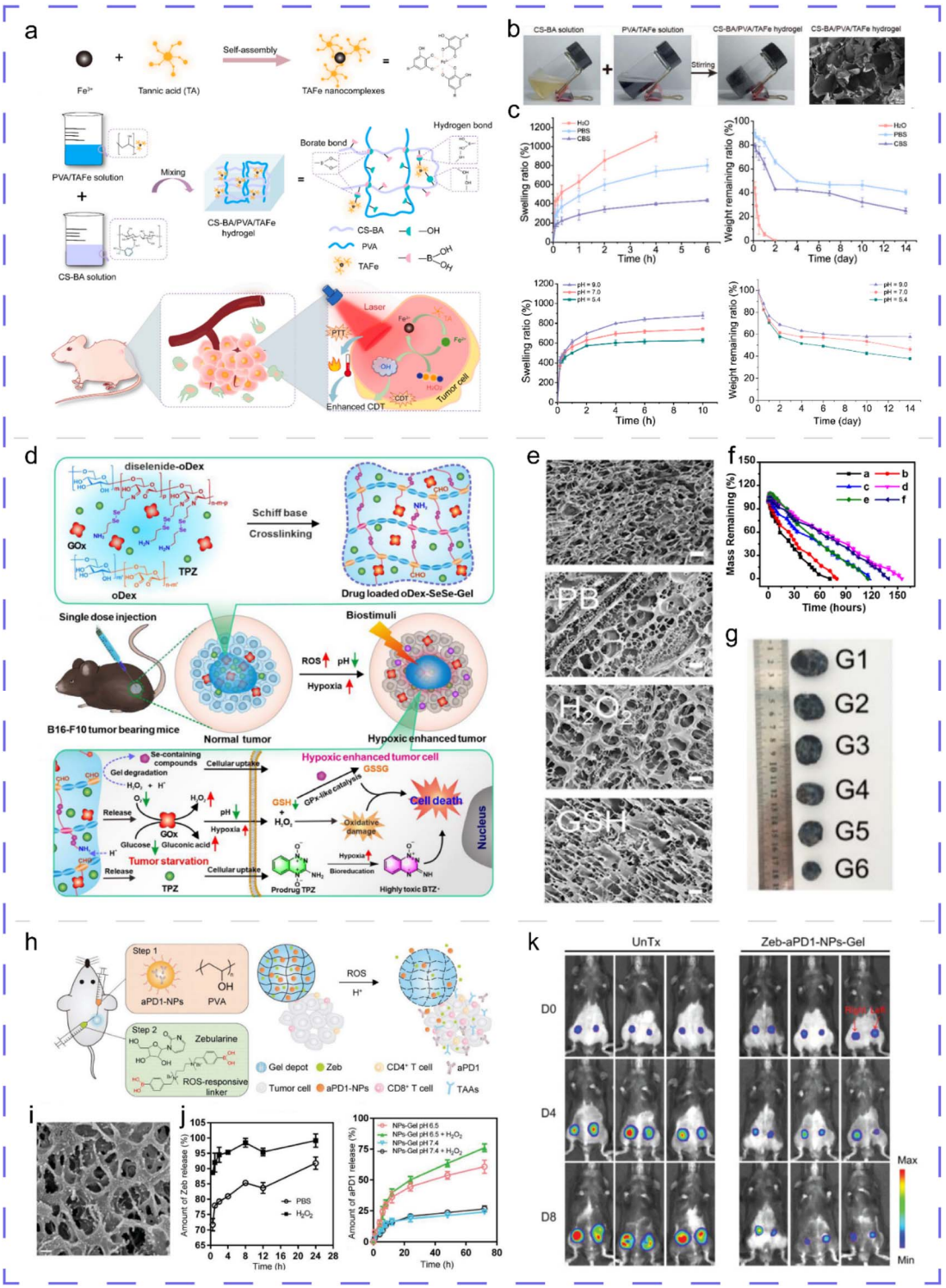

Fig. 7 (a) Schematic overview of TAFe synthesis, CS-BA/PVA/TAFe hydrogel formation, and its combined PTT/CDT tumour therapy. (b) Photograph of CS-BA and PVA/TAFe solutions (1 : 1) forming CS-BA/PVA/TAFe hydrogel, with its SEM micrograph. (c) Swelling and degradation kinetics of CS-BA/PVA/TAFe hydrogel in varied solvents and pH-adjusted PBS. Adapted with permission from ref. 166, Copyright 2024, Elsevier Ltd. (d) Schematic diagram of drug-loaded multi-responsive oDex-SeSe-Gel for enhancing local starvation- and hypoxia-activated melanoma chemotherapy. (e) SEM of lyophilised oDex-SeSe-Gel mesh and its degradation at pH 6.8 PB, 100 μM H_2O_2 or 100 μM GSH. (f) Remaining mass of oDex-SeSe-Gel incubated under different conditions over time. (g) *In vivo* antitumour efficacy: representative photographs of tumours after different treatments. Adapted with permission from ref. 173, Copyright 2023, Elsevier BV. (h) Schematic and characterisation of injectable *in situ* formed ROS/H^+ dual bioresponsive gel depots. (i) Representative Cyro-SEM image of hydrogel loaded with αPD-1 NPs. (j) The release profiles of Zeb and αPD-1 were measured from the same NPs-loaded gel under different conditions. (k) *In vivo* bioluminescence imaging of bilateral B16F10 tumours shows systemic immune responses over time after local delivery of Zeb-αPD-1-NPs-Gel. Adapted with permission from ref. 179, Copyright 2019, Wiley-Blackwell.

with dihydroartemisinin (DHA), Fe^{3+} chelates, and protoporphyrin IX (PpIX). Upon entering the acidic tumour microenvironment, the microneedle's network structure rapidly degrades. This degradation releases Fe^{2+}, which catalyses the cleavage of the endoperoxide bridge within the DHA molecule. The process triggers the on-demand generation of a ROS burst. Consequently, the system exhibits potent synergistic killing of B16 melanoma cells.

5.2. Redox-responsive hydrogels

GSH, a pivotal intracellular antioxidant, plays a central role in maintaining cellular redox homeostasis. Under physiological conditions, the GSH concentration in the cytoplasm of normal cells ranges from 2 to 10 mM, whereas the ECM contains only 2–20 μM, establishing a pronounced transmembrane concentration gradient. Notably, tumour cells exhibit GSH levels approximately fourfold higher than those in normal cells, creating a highly reducing intracellular environment. In contrast, the extracellular TME is oxidised due to excessive accumulation of ROS.[169,170] This unique property establishes redox-responsive hydrogels as an intelligent platform for tumour-targeted drug delivery. By sensing variations in GSH concentration, these systems can trigger precise drug release, achieving selective intracellular delivery within tumour cells.

The design principle of redox-responsive hydrogels centres on the incorporation of reduction-sensitive chemical bonds, among which disulfide bonds (–S–S–) are the most well-established. I Beyond disulfide bonds, selenium-containing bonds, particularly diselenide bonds, have emerged as a novel strategy for designing such hydrogels due to their unique redox activity. Within the GSH-rich microenvironment of a tumour cell, disulfide bonds are cleaved. This cleavage reduces crosslink density, causing the polymer network to transition from a compact state to a swollen or even degraded state. In contrast, the structure remains stable in an oxidised extracellular environment. This structural behaviour directly governs the drug release profile. A rapidly degrading network typically results in burst or fast release, a characteristic desirable for chemotherapeutics that require swift attainment of a lethal concentration. Conversely, a slowly swelling network confers sustained-release properties, making it suitable for protein-based drugs, such as glucose oxidase, that require prolonged activity.[171,172] Drawing on this principle, researchers have designed various intelligent platforms for CM. For example, to cope with the complex tumour microenvironment, Ding *et al.*[173] developed a dual redox-responsive hydrogel through oxidised dextran-diselenide crosslinking, co-encapsulating glucose oxidase (GOx) and tirapazamine (TPZ). This system exhibits GSH peroxidase (GPx)-like cascade catalytic activity, high drug loading efficiency, and rapid responsiveness to GSH: under 10 mM GSH, the cumulative release of GOx and TPZ reached 86% and 95%, respectively, demonstrating significant potential in GSH-amplified starvation-hypoxia synergistic therapy (Fig. 7d–g). Vu *et al.*[174] engineered a water-soluble PEG-based disulfide crosslinker (DTz-DS-PEG) by inserting a PEG spacer between two disulfide bonds and functionalizing the termini with tetrazine groups. A reduction-sensitive hydrogel was subsequently fabricated *via* inverse IEDDA reaction using alginate-norbornene derivatives, DOX, and DTz-DS-PEG. The hydrogel exhibited no significant toxicity in fibroblasts. The crosslinker itself also demonstrated good biocompatibility, rendering the system a safe carrier platform for the targeted and controlled release of DOX. To achieve precise subcellular targeting, Mei *et al.*[175] developed a redox-responsive hydrogel loaded with the mitochondrial-targeting peptide KLAK and niclosamide. They constructed this hydrogel (Pep-CS-LND) using self-assembling peptides (Nap-GFFYK), anticancer agent niclosamide (LND), and mitochondrial-targeting peptides (KLAK) as key building blocks. The hydrogel exhibits outstanding biocompatibility, high drug-loading capacity, and intrinsic mitochondrial-targeting capability. Upon stimulation with 10 mM GSH, approximately 75% of the LND-KLAK complex was released, effectively inducing mitochondrial dysfunction and triggering caspase-dependent apoptosis in tumour cells, thereby enhancing therapeutic outcomes.

5.3. ROS-responsive hydrogels

ROS are unavoidable by-products of cellular aerobic metabolism, primarily generated in the mitochondrial electron transport chain, NADPH oxidase complexes, and the endoplasmic reticulum oxidative folding system.[176] Key ROS species include superoxide anion ($^{\bullet}O_2^-$), hydroxyl radical ($^{\bullet}OH$), hydrogen peroxide (H_2O_2), and singlet oxygen ($^1O_2$). Excessive ROS production induces oxidative damage to intracellular DNA, lipids, and proteins, which can trigger genetic mutations and initiate carcinogenesis. Notably, tumour cells exhibit significantly elevated endogenous ROS levels compared to normal cells, creating a unique biochemical trigger for targeted therapy. Leveraging this disparity, sensitive groups within the hydrogel undergo oxidative cleavage under high levels of ROS. This process shifts the network from a dense state to a loose, swollen, or even fully degraded structure. Such a transformation not only enables controlled drug release but also gives rise to distinct release patterns depending on the rate of structural change. These patterns range from a slight burst release driven by surface diffusion, to sustained release as the network slowly disintegrates, and ultimately to on-demand pulse release triggered at a specific ROS threshold.[177,178]

Ruan *et al.*[179] developed an ROS-responsive hydrogel that rapidly degrades in the high-ROS TME, enabling the co-delivery of zebularine and αPD-1. This system reshapes epigenetic profiles and activates $CD8^+$ T cells, thereby potentiating systemic antitumour immunity against melanoma (Fig. 7h–k). Gao *et al.*[180] constructed an ROS-responsive *Dendrobium* polysaccharide-based hydrogel (MnP@DOP-Gel) that facilitates sustained release of manganese-pectin microspheres (MnP) within the postoperative inflammatory milieu. By activating the cGAS-STING signalling pathway, the system directly induces immunogenic cell death (ICD) and synergistically enhances dendritic cell and macrophage-mediated antitumour immune responses, effectively suppressing both local recurrence and distant metastasis of melanoma. This process achieves long-

term activation of the cGAS-STING pathway, thereby remodelling the immune microenvironment. Zhang *et al.*[107] designed a conjugated polymer hydrogel, designated aCD47/Ce6@PPG, that extends this approach. Upon exposure to the ROS surge generated by PDT, the hydrogel undergoes rapid dissociation and on-demand release. This process simultaneously delivers therapeutic agents and scavenges excess ROS. By inducing ICD and blocking the CD47-SIRPα pathway, the system establishes a closed loop linking local treatment to systemic immune activation.

5.4. Enzyme-responsive hydrogels

Enzymes play a pivotal role in regulating cellular and molecular microenvironmental homeostasis and driving both physiological and pathological processes.[181] Notably, tumour cells frequently overexpress certain enzymes compared to their normal counterparts, rendering these enzymes ideal endogenous triggers for site-specific, enzyme-mediated drug release.[182,183] Enzyme-responsive hydrogels are typically designed by incorporating enzyme-labile bonds, such as ester or peptide linkages, into their network architecture. This involves integrating specific enzymatic cleavage sites into the peptide sequences of the hydrogel building blocks. These sites can be recognised and cleaved by corresponding enzymes, like esterases or proteases. The subsequent peptide cleavage alters the hydrogel's conformation, ultimately leading to its disintegration and the controlled release of encapsulated therapeutic agents.[34]

Based on the design of enzyme-cleavable sites, the network structure of hydrogels can undergo distinct transformation patterns.[184] These patterns entail enzymatic cleavage of either the crosslinks or the backbone that constitute the gel matrix, resulting in fragmentation of the 3D network and progressive collapse of the hydrogel. Alternatively, enzymes may remove side chains or partial branches, which reduces crosslinking density.[185] This leads to network swelling and increased pore size, thereby accelerating the diffusion of encapsulated drugs. Another mechanism involves a gel–sol transition. In supramolecular peptide hydrogels, enzymatic cleavage can disrupt the noncovalent driving forces of molecular assembly (*e.g.*, π–π stacking), leading to a shift from a gel to a solution state.[186] The resulting changes in network structure directly determine drug release kinetics, enabling profiles such as burst release, sustained release, or on-demand triggered release. Building on these principles, researchers have engineered various enzyme-responsive hydrogels for precision oncology. A range of enzymes has been exploited to modulate hydrogel formation and degradation, including MMPs, alkaline phosphatase (ALP), carboxylesterase (CES), lysyl oxidase, proteases, β-lactamase, and transglutaminase.[187] MMPs, a class of endopeptidases that cleave peptide bonds, play a critical regulatory role in tumour angiogenesis, invasion, and metastasis. Chen *et al.*[188] developed an MMP-2/pH dual-responsive hydrogel co-loaded with nanohydroxyapatite (nHA) and the lactate dehydrogenase inhibitor GNE (Fig. 8a–c). This system effectively suppresses lactate metabolism in melanoma cells and directly induces tumour cell death, thereby significantly enhancing antitumour immune responses. Jia *et al.*[189] designed a "core–shell" nanocarrier: the outer shell consists of negatively charged PEG-histidine (PEG-His), while the inner core is based on the peptide sequence PLGVRKLVFF, with the chemotherapeutic agent berberine (BBR) and the photosensitizer Ce6 conjugated to either terminus. Building on these principles, researchers have engineered various enzyme-responsive hydrogels for precision oncology. In one design, an acidic pH triggers the shedding of an outer shell through surface network reconstruction. This exposes a core cleaved specifically by MMP-2, an enzyme highly expressed in tumours. The subsequent network degradation enables the precise release of two therapeutic agents: the chemotherapeutic drug BBR and the photosensitizer Ce6. This strategy achieves a synergistic effect by combining chemotherapy with PDT. The catalytic activity of enzymes overexpressed in tumour cells can be harnessed to trigger the *in situ* self-assembly of therapeutic agents. Wu *et al.*[190] fabricated a carrier-free, enzyme-responsive hydrogel, LND-1p-ES, composed of chlorambucil (LND) linked *via* an amide bond to a glycine–phenylalanine–phenylalanine–tyrosine (GFFY) motif, followed by phosphotyrosine (pY) and succinic acid monoester (ES). By exploiting the enzymes ALP and CES, which are overexpressed in tumour cells, the system first triggers molecular self-assembly into a nanofibre network, leading to gel formation. The subsequent degradation of this network by proteases enables prolonged and controlled drug release. This approach offers both high selectivity and low systemic toxicity. In another study, Chen *et al.*[191] designed an enzyme-responsive, thermosensitive polypeptide hydrogel co-encapsulating DOX and dual immune checkpoint inhibitors (αCTLA-4 and αPD-1). In the presence of proteinase K, the hydrogel rapidly degrades, accelerating drug release and enabling sustained local delivery within tumours. By inducing ICD and blocking the CTLA-4/PD-1 signalling axis, this platform potentiates systemic antitumour immunity and effectively suppresses postoperative tumour recurrence.

5.5. Thermosensitive hydrogels

Temperature serves as a key external stimulus that triggers structural transitions in injectable polymeric hydrogel networks. These hydrogels are typically composed of hydrophilic and hydrophobic segments linked *via* covalent or physical crosslinking, with their macroscopic responsiveness primarily determined by the relative ratio of these domains.[192,193] At low temperatures, hydrophilic groups form hydrogen bonds with surrounding water molecules, leading to hydration and swelling, resulting in a free-flowing sol state. Upon injection into tumour or peritumoural tissues, exposure to physiological temperature (37 °C) disrupts these hydrogen bonds, inducing dehydration, contraction, and a phase transition from sol to gel. This temperature-mediated physical crosslinking facilitates rapid gel network formation and confers long-term structural stability to the material *in vivo*. Based on this phase transition, thermosensitive hydrogels exhibit unique drug-release kinetics. Immediately after gelation, the rapid

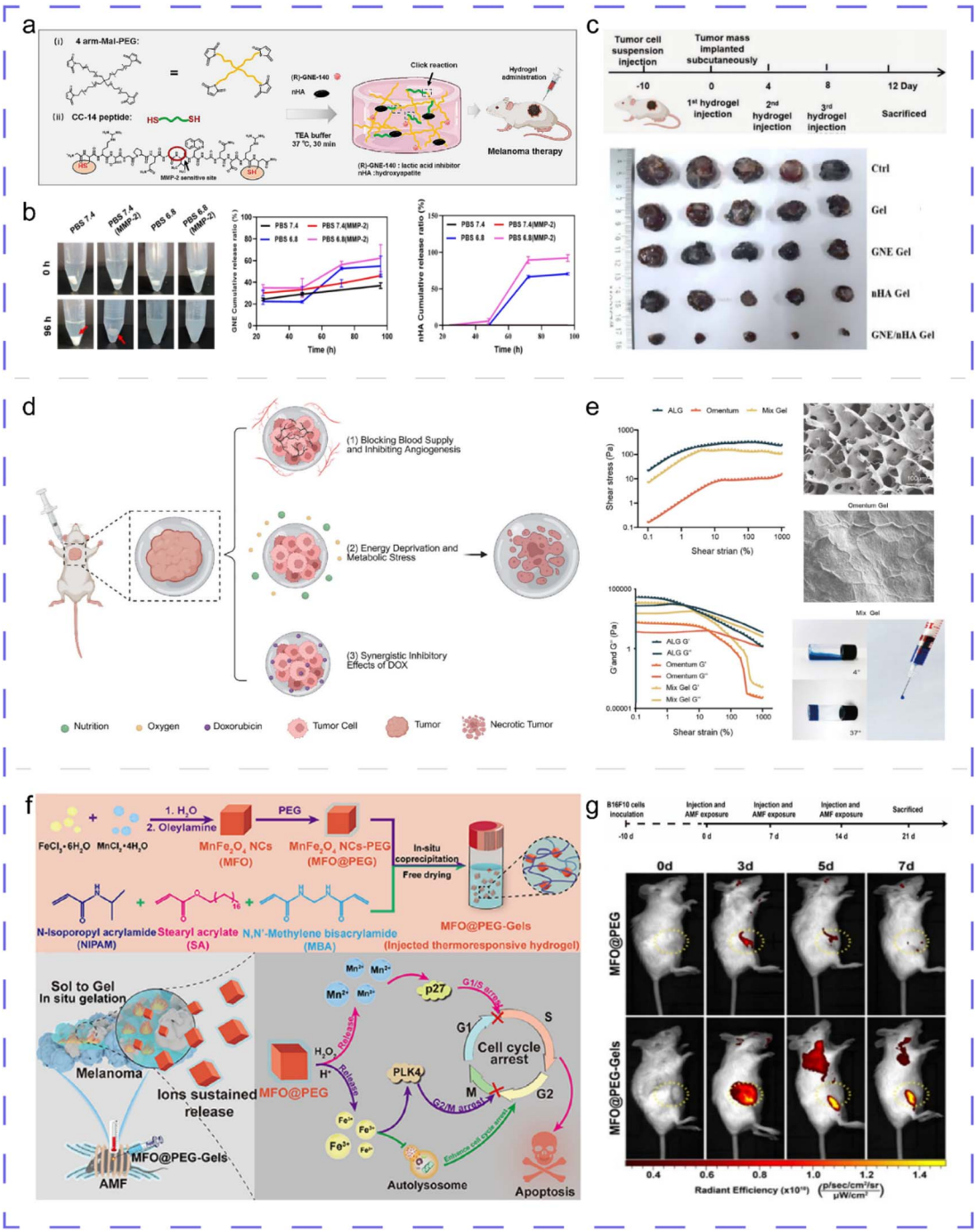

Fig. 8 (a) Schematic images of the hydrogel preparation process and application. (b) Hydrogel degradation behaviour and the cumulative release profiles of GNE/nHA under different conditions. (c) Digital images of tumour after different treatments. Adapted with permission from ref. 188, Copyright 2024, Elsevier BV. (d) Proposed mechanisms of tumour inhibition by DOX-Mix Gel. (e) Characterisation of Mix Gel. Adapted with permission from ref. 195, Copyright 2025, John Wiley and Sons Ltd. (f) Schematic illustrations of the synthesis procedure of magnetic bimetallic hydrogel and its application in ion-interferential cell cycle arrest for melanoma treatment. (g) Schematic illustration of intratumoural MFO@PEG-Gel injection followed by alternating magnetic field exposure. Adapted with permission from ref. 201, Copyright 2024, Elsevier.

contraction of the network helps suppress an initial burst release. As the hydrogel persists in the body at physiological temperatures, the encapsulated drug is released primarily by diffusion or through gradual gel degradation, resulting in a sustained release profile.[194] Moreover, by modulating the pore size of the gel network or incorporating responsive nanocarriers, on-demand release can be achieved in response to specific microenvironmental signals.

To reduce the systemic toxicity associated with conventional chemotherapy, researchers have explored various design

strategies based on thermosensitive platforms. Gong *et al.*[195] developed a bioactive hydrogel platform using a decellularised omental matrix (Omentum Gel) as a natural scaffold, reinforced with sodium alginate to enhance mechanical integrity. After loading DOX, the system demonstrated excellent biocompatibility, tunable network structure, and potent antitumour efficacy *in vitro* and *in vivo* (Fig. 8d and e). Li *et al.*[196] developed an injectable, long-acting nanohybrid temperature-sensitive hydrogel, designated NanoCD@Gel. This system employs albumin nanoparticles (NanoCD) as a carrier, co-loaded with the immunogenic chemotherapeutic agents curcumin and DOX. These drug-loaded nanoparticles are embedded within a thermosensitive Pluronic P407 hydrogel matrix. The formulation is designed for post-operative immunogenic chemotherapy. It enables localised, sustained drug release and promotes immune activation. This strategy aims to inhibit tumour recurrence and metastasis following surgery. In another study, Kloepping *et al.*[197] designed a localised delivery system based on a polyethene glycol–polylactic-*co*-glycolic acid (PEG–PLGA) thermosensitive hydrogel for the sustained release of triphenylphosphine derivatives (TPP). The formulation remains injectable at 4 °C and undergoes rapid gelation at body temperature, achieving more than tenfold drug enrichment at the target site and continuous release over 48 hours. Leveraging this precise spatial retention and controlled release profile, TPP persistently disrupts mitochondrial metabolism in melanoma cells, induces lipid peroxidation and thiol oxidative stress, and significantly inhibits tumour progression in murine models, all while exhibiting minimal systemic toxicity.

5.6. Magnetic-responsive hydrogels

Magnetic-responsive hydrogels have attracted much attention due to their unique advantages of remote control and precise space-time regulation.[198] The typical fabrication strategy involves incorporating magnetic nanoparticles, such as iron oxide-based magnetite or maghemite, or cobalt and nickel ferrites, into a thermoresponsive hydrogel matrix. When exposed to an external magnetic field, the response mechanisms of such composite materials can be engineered across three key dimensions. The first involves changes in the network structure. Magnetic nanoparticles can generate a magnetic hyperthermia effect under an alternating magnetic field, inducing volume phase transitions, such as swelling or shrinkage, or sol–gel transitions in thermosensitive matrices. This field can also be used to remotely guide the targeted migration and accumulation of the entire DDS within the body.[199,200] The second dimension is the modulation of release behaviour. Leveraging changes in network structure enables switching between various drug-release modes, ranging from suppressed-burst to sustained to on-demand pulsatile release. The third is applications in disease treatment. Through these synergistic mechanisms, magnetic-responsive hydrogels offer an intelligent platform for combined chemical and physical therapies, particularly in the treatment of malignant tumours.

In recent years, through sophisticated nano-gel interface design, researchers have introduced numerous innovations within these dimensions. For instance, to achieve synergy between network degradation and cyclical treatment schedules, Li *et al.*[201] encapsulated Mn–Fe oxide nanoblocks within an injectable poly(ethylene glycol) (PEG)-based hydrogel (MFO@PEG-Gels). Under an alternating magnetic field, the system generates localised heat through magnetic hyperthermia, triggering a sol–gel phase transition and promoting sustained release of Mn^{2+} and Fe^{3+} ions. These ions selectively arrest the cell cycle at the G1/S and G2/M checkpoints, respectively, leading to synchronised cell cycle inhibition and efficient induction of apoptosis in melanoma cells (Fig. 8f and g). Adam[202] synthesised a PCLA-PEG-PCLA thermosensitive hydrogel using $Zr(acac)_4$ as a catalyst and incorporated 10 nm superparamagnetic iron oxide nanoparticles (MIONs) *via* co-precipitation. This design not only imparts the gel with excellent magnetic targeting and magnetothermal conversion capabilities to enable on-demand release of anti-tumour drugs, but also, owing to its favourable biocompatibility, establishes a versatile platform for long-acting, precise localised drug delivery.

5.7. Light-responsive hydrogels

Light, as a non-invasive external stimulus, enables both *in situ* polymerisation and spatiotemporally precise triggering of anticancer drug release in light-responsive hydrogels.[203] These intelligent systems are typically categorised according to the excitation wavelength into three classes: NIR-, visible light-, and UV-responsive networks.[204] They drive changes in network structures through distinct physicochemical mechanisms, which in turn govern drug release behaviour.

NIR light-responsive systems typically rely on photothermal conversion agents that induce local hyperthermia, leading to reversible swelling, shrinkage, or phase transition of the gel network. This enables on-demand pulsatile drug release and PTT. Liu *et al.*[205] developed an injectable hydrogel based on manganese-doped bioactive glass and sodium alginate, referred to as BG-Mngel. Upon exposure to 808 nm NIR irradiation, the material rapidly heats up, inducing local network contraction. This enables mild PTT while simultaneously delivering the immune modulator α-PD-1. In a B16F10 melanoma model, this combined approach resulted in marked tumour suppression (Fig. 9a–c). Chang *et al.*[206] co-encapsulated gold nanorods and DOX into an oxidised carboxymethyl cellulose/P(NIPAM-*co*-AH) cross-linked network, using the NIR photothermal effect to induce a low-temperature phase transition within the hydrogel network enables remotely controlled on-demand drug release while reinforcing the synergistic effect of photothermal and chemotherapy. This approach exemplifies a dual-purpose design strategy that achieves both high efficacy and low toxicity.

In contrast, UV- and visible-light-responsive systems typically rely on photochemical reactions that trigger irreversible network degradation or a reduction in crosslink density, thereby enabling sustained drug release or programmed delivery. Zhou *et al.*[207] encapsulated CAR-T cells into an injectable GelMA hydrogel, which was implanted directly into tumours following rapid UV-triggered gelation. This design uses

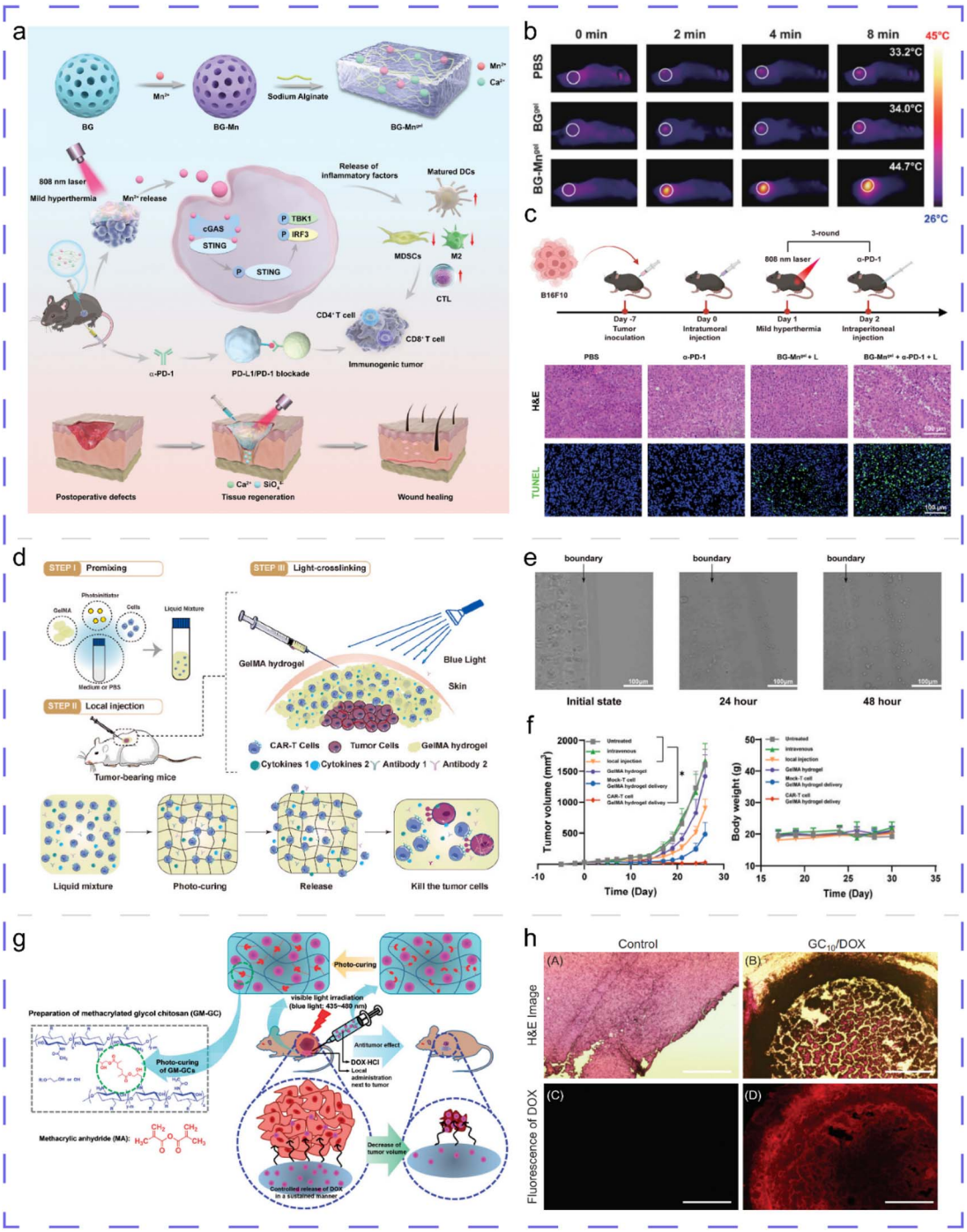

Fig. 9 (a) Schematic illustration showing a bioactive injectable hydrogel (BG-Mn gel) for the regulation of tumour metastasis and wound healing for melanoma. (b) *In vivo* infrared thermal images of the B16F10 melanoma-bearing mice upon laser irradiation. (c) Schematic of long-term immune response assessment and representative H&E/TUNEL images of residual tumours after combination therapy in B16F10 tumour-bearing C57BL/6 mice. Adapted with permission from ref. 205, Copyright 2024, Wiley-VCH Verlag. (d) Schematic of an injectable hydrogel delivery system installation loaded with CAR-T cells. (e) The migration of CAR-T cells from hydrogels was measured by microimaging. (f) Average tumour growth and mouse body-weight curves for various treatment groups. Adapted with permission from ref. 207, Copyright 2022, Elsevier BV. (g) Schematic of peritumoural GC10/DOX injection and its proposed mechanism for enhanced cancer therapy. (h) H&E-stained images of dissected tumour tissues and fluorescence of DOX in the tumour tissues. Adapted with permission from ref. 208, Copyright 2022, MDPI (Basel, Switzerland).

ultraviolet light to trigger *in situ* crosslinking of the network, forming a delivery barrier that enables sustained release of T cells within the local tumour environment. This approach overcomes the challenge of inadequate T cell homing associated with conventional intravenous injection (Fig. 9d–f). Additionally, visible light offers advantages for rapid prototyping owing to its higher biosafety profile. Hyun *et al.*[208] employed visible light to rapidly cure a glycol chitosan-based hydrogel

(GC/CD/PTX) within 10 seconds. By encapsulating a paclitaxel (PTX)-β-cyclodextrin complex, this network substantially improves drug solubility. The dense structure of the crosslinked matrix ensures sustained and stable PTX release over 7 days, offering a straightforward and low-toxicity clinical strategy for local chemotherapy (Fig. 9g and h).

In summary, by precisely modulating structural changes within the network, for instance, through phase transition-induced contraction or degradation, photoresponsive hydrogels enable diverse drug release profiles ranging from burst and sustained release to on-demand pulsatile patterns. In cancer therapy, these materials have demonstrated versatile applications, including light-controlled immune activation, cell delivery, and localised chemotherapy. Such capabilities establish a robust foundation for the development of integrated precision treatment platforms.

6. Application of hydrogel DDS in CM treatment

The 3D porous architecture of hydrogels confers exceptional drug encapsulation capacity. Upon incorporation into the hydrogel matrix, therapeutic agents can be released in a sustained, controlled manner by precisely modulating structural parameters, such as pore size and crosslinking density, which govern the diffusion kinetics of the loaded drugs. Furthermore, owing to their inherent hydrophilicity, excellent biocompatibility, and tunable biodegradability, hydrogels serve not only as promising wound dressings but also as versatile platforms for cancer therapy. In melanoma treatment, hydrogel-based systems have been extensively investigated for multiple therapeutic strategies, including targeted delivery of chemotherapeutic agents, enhancement of radiotherapy efficacy through radiosensitisation, delivery of photosensitizers or photothermal agents for photodynamic and photothermal therapies, and spatiotemporally controlled release of immunomodulators to potentiate immunotherapeutic responses. These multifunctional capabilities position hydrogels as advanced localised delivery systems with significant translational potential in melanoma management.

6.1. Hydrogel-based delivery of chemotherapeutic agents for melanoma therapy

Traditional chemotherapy delivery systems face significant challenges, including poor tumour penetration, high systemic toxicity, and the propensity to induce drug resistance, all of which severely limit their clinical efficacy.[209] Hydrogel materials, with their high water content, excellent mechanical compliance, and microstructural similarity to the ECM, not only enable the reconstruction of the tumour microenvironment but also offer an ideal platform for addressing these challenges through their tunable physicochemical properties.

Therefore, the development of advanced carriers with high drug loading capacity and spatiotemporally controlled release profiles is of critical importance. Hydrogels, characterised by high water content, excellent mechanical compliance, and a microstructure resembling the ECM, can effectively modulate the TME while enabling sustained and localised drug release. Their inherent biocompatibility and tenable degradability have positioned hydrogels as a leading platform in next-generation drug delivery research.

To address the diverse physicochemical properties of chemotherapeutic agents, researchers have achieved high-efficiency drug loading by precisely tailoring the hydrogel network structure. Commonly used chemotherapeutic agents in melanoma treatment include dacarbazine, temozolomide, nitrosoureas, carboplatin, and taxane derivatives.[210] To address the challenge of loading hydrophobic chemotherapeutic agents, Mathiyalagan *et al.*[211] constructed a host scaffold based on β-cyclodextrin (βCD)-functionalized HA. By leveraging the hydrophobic inclusion capacity of the βCD cavity, they successfully loaded the natural bioactive component, the triterpenoid saponin (CK), achieving targeted inhibition against B16F10 melanoma cells (Fig. 10a–d). For metal-based drugs such as cisplatin, Miao *et al.*[212] co-encapsulated the agent with single-atom iron-carbon nanozymes within a β-CD-*g*-PEGMA brush-like network. By utilising the high-density branched polymer brush, they achieved efficient drug retention and stable loading, thereby laying the groundwork for subsequent multimodal combination therapy.

Building on the achievement of high loading efficiency, aligning drug release behaviour with the therapeutic window is critical for ensuring efficacy. Li *et al.*[213] developed an in situ-forming hydrogel based on tetra-arm polyethene glycol thiol (PEGSH) and polyethene glycol diacrylate (PEGDA), designated 4-PEG-SH/PEG-DA. This system enables co-delivery of DOX and R837 within the hydrogel matrix. Following local injection, the hydrogel provides sustained dual-drug release, directly inducing melanoma cell death while simultaneously activating innate and adaptive immune responses, thereby demonstrating strong potential for combination therapy. Furthermore, to achieve more precisely controlled release, designing smart hydrogels that respond to the tumour microenvironment has emerged as a key research focus. Sun *et al.*[214] developed a modified natural polysaccharide-based hydrogel platform (SCOD) using oxidised dextran (OD) and *N*-succinyl chitosan (SC), crosslinked *via* dynamic Schiff base bonds, with DOX as the model therapeutic. In the acidic tumour microenvironment, these bonds are cleaved, enabling pH-responsive, precise drug release. In both *in vitro* and *in vivo* melanoma models, this formulation demonstrated antitumor efficacy that was significantly superior to free DOX administered intravenously at equivalent doses. This work effectively showcases the advantages of intelligent, responsive DDS.

6.2. Hydrogel-based delivery of radiosensitizers for melanoma therapy

Radiotherapy serves as a therapeutic strategy capable of curative or palliative intervention in melanoma patients, offering effective local control for specific lesions such as lentigo maligna, regional lymph node metastases, and bone or brain metastatic sites.[215,216] To overcome the limited selectivity of traditional

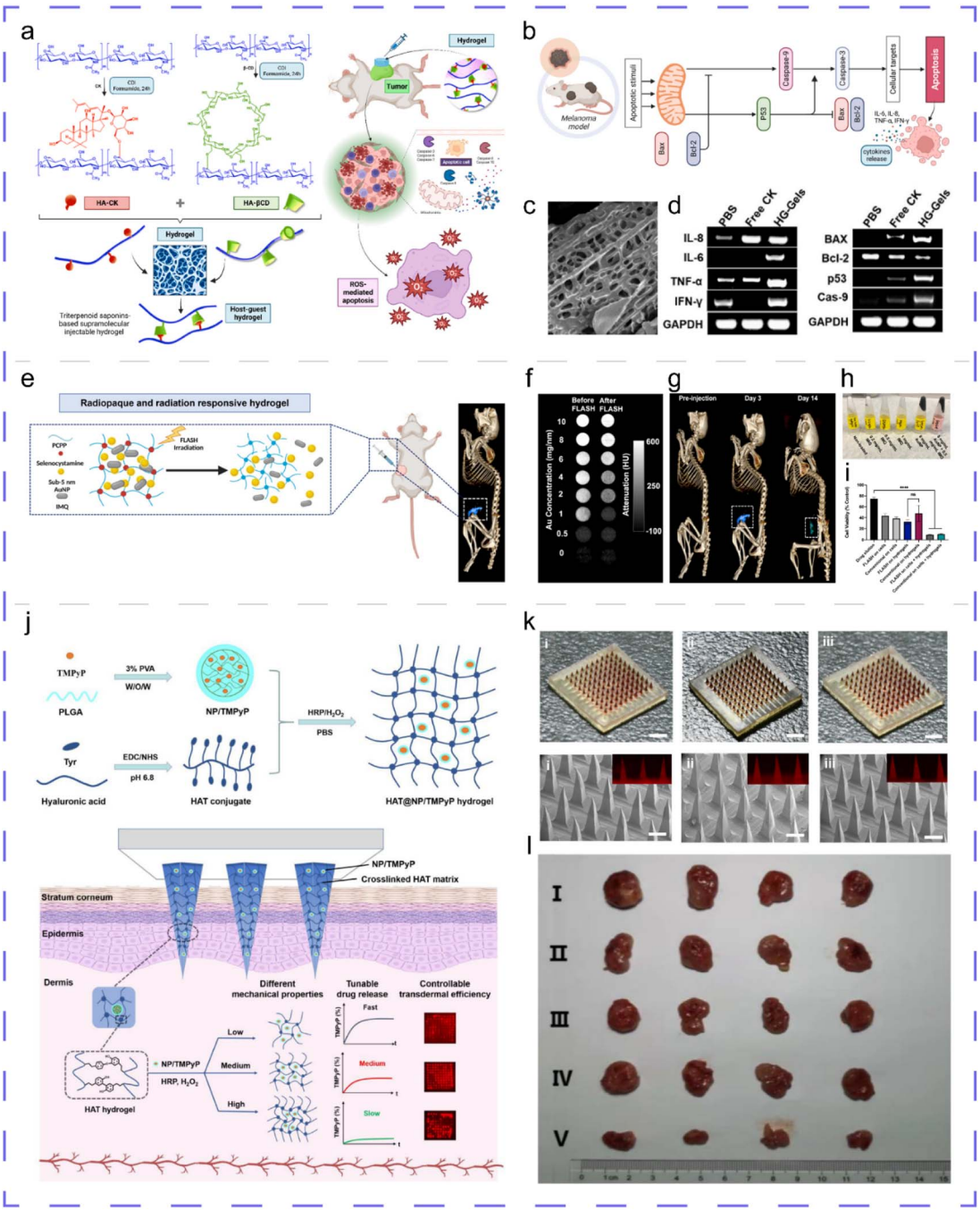

Fig. 10 (a) Schematic illustration of an injectable supramolecular hydrogel and the mechanism of the injectable hydrogel system. (b) and (d) The expression of proinflammatory cytokines and apoptosis induced gene levels in mouse serum was analysed using semi-quantitative RT-PCR aftertreatments. (c) FE-SEM images of HG-Gel surface micromorphology after lyophilisation. Adapted with permission from ref. 211, Copyright 2024, Elsevier BV. (e) Schematic representation of the FLASH-RT triggered release of IMQ drug and AuNP from the AuNP-IMQ hydrogel. (f) CT phantom scans of hydrogels before and 7 days after FLASH-RT. (g) Representative 3D CT images of a mouse with the hydrogel highlighted in blue. (h) Digital images of the synthesis process of the AuNP-IMQ hydrogel. (i) Viability of B16–F10 cells at 48 h after receiving different treatments. Adapted with permission from ref. 219, Copyright 2023, American Chemical Society. (j) Schematic illustration of transdermal delivery of TMPyP with different mechanical properties, tunable drug release, and controllable transdermal efficiency. (k) Optical and SEM images of three types of HAT@NP/TMPyP-MNs. (l) Diagram of dissected A375-xenografted tumours in mice at the end of different treatments. Adapted with permission from ref. 230, Copyright 2024, Elsevier BV.

radiotherapy for tumour tissues and enhance local therapeutic effects, researchers have used hydrogels as delivery platforms. By leveraging the unique hydrophilic, porous network of hydrogels through precise design, this approach enables effective loading and controlled release of radionuclides and radiosensitizers. Consequently, it achieves potent radiosensitisation specifically at the tumour site.

First, from a design perspective, hydrogels must be tailored to the physicochemical properties of various radionuclides and radiosensitizers. For example, ^{131}I stands out due to its favourable physical decay properties, established clinical safety profile, and cost-effectiveness, rendering it one of the most widely utilised radionuclides in current practice.[217] To address this need, Zhang *et al.*[218] developed a multifunctional hydrogel co-loaded with gold nanoclusters (GNPs), DOX, and ^{131}I-labeled methoxy poly(ethylene glycol) (mPEG). This system leverages the dual role of gold nanoparticles (GNPs) as both radiosensitizers and photosensitive agents. The system cleverly accommodates the distinct properties of its components through rational design. First, it achieves adaptive loading by labelling ^{131}I with mPEG, while co-encapsulating hydrophobic DOX and GNPs within the hydrogel network. This design effectively solves the challenge of delivering hydrophobic drugs. Second, the system ensures matched release and enhanced efficacy. By leveraging the radiosensitising properties of GNPs, it amplifies tumour cell killing during radiotherapy. At the same time, it enables tumour-microenvironment-responsive and controlled release of DOX. This allows the chemotherapeutic release profile to align with the radiotherapy schedule, ultimately achieving synergistic effects through combined radiotherapy, phototherapy and chemotherapy.

Furthermore, researchers used a hydrogel design to achieve the sustained release of immunomodulators. This approach was designed to precisely match the therapeutic window for immunotherapy. Dong *et al.*[219] innovatively integrated FLASH-RT with immunotherapy by designing a radiopaque, FLASH-RT-responsive hydrogel loaded with the TLR7 agonist imiquimod (IMQ). This system enables the localised loading and long-term controlled release of the IMQ through intratumoral injection. This sustained release strategy ensures that the immune adjuvant persistently activates local antitumour immunity following tumour ablation by FLASH-RT. The synergistic effect of this combination markedly inhibited melanoma growth and prolonged survival (Fig. 10e–i).

To further inhibit metastases and enable real-time monitoring of therapeutic efficacy, the material design must also incorporate imaging capabilities and facilitate deep tissue penetration. Cui *et al.*[220] fabricated a composite hydrogel (^{225}Ac-FeTA-PEG-R837) by crosslinking ^{225}Ac-labeled iron tannic acid nanoparticles (FeTA) with 4-arm PEG-thiol (4-ArmPEG-SH) in the presence of the immune adjuvant R837. This system enabled dual-modal imaging *via* iron-based MRI and radionuclide tracking, allowing visualisation of the treatment process. The incorporation of FeTA nanoparticles not only enhanced the mechanical properties of the hydrogel but also improved its intratumoral penetration. When combined with immune checkpoint blockade, this approach effectively activated systemic antitumor immunity and inhibited distant metastasis.

6.3. Hydrogel-mediated PTT and PDT for melanoma

Light-mediated technologies are increasingly enabling precise interventions in oncology, infection management, and tissue regeneration. Among these approaches, PTT and PDT have emerged as two of the most representative non-invasive therapeutic modalities.[221,222] PTT relies on photothermal agents to convert light energy into heat.[223,224] whereas PDT uses photosensitizers to generate ROS under light irradiation for tumour ablation. However, several challenges impede the clinical translation of these phototherapies. These include the tendency of hydrophobic phototherapeutic agents to aggregate, the limited efficacy of PDT in the hypoxic tumour microenvironment, and the inability of monotherapy to achieve complete tumour eradication.[225,226] Hydrogels offer an ideal platform for the precise delivery and controlled release of phototherapeutic agents, owing to their tunable drug-loading microenvironment and responsiveness to tumour microenvironments. To achieve efficient thermal ablation of deep-seated tumours, researchers have leveraged the deep-tissue penetration of the second NIR window (NIR-II, 900–1400 nm) to develop polymer-based photothermal agents.[227] However, hydrophobic agents like polyaniline (PANI) are prone to aggregation and deactivation in physiological environments. To address this, Huang *et al.*[228] designed an injectable, self-healing GG@PANI(Fe)-borax hydrogel by incorporating iron-doped PANI into a guar gum backbone. At the design level, iron-doped polyaniline was incorporated into a guar gum matrix. The spatial confinement effect of the hydrogel network prevented PANI aggregation, addressing the stability issues of hydrophobic photothermal agents in physiological environments. For loading, PANI(Fe) was anchored within the gel network through chemical and physical interactions, ensuring uniform dispersion. Regarding release and action, upon NIR-II irradiation, the system benefited from the protective effect of the gel network on PANI(Fe), resulting in stable and efficient photothermal conversion. In terms of therapeutic efficacy, the localised high temperature achieved complete tumour ablation while simultaneously inhibiting wound infection and promoting angiogenesis. This approach integrates tumour eradication with postoperative tissue repair within a single platform.

PDT is highly dependent on the photosensitizer's delivery efficiency and the oxygen concentration at the tumour site. To address the strong hydrophobicity and short duration of action of the traditional photosensitizer Ce6, Tang *et al.*[229] drew inspiration from natural silk fibroin. They designed a hydrophilic backbone using methacrylic anhydride-modified silk fibroin, which efficiently loads the photosensitizer Ce6 through hydrophobic interactions to form an SF-MA/Ce6 composite hydrogel. Under NIR light irradiation, this system not only generates substantial ROS *via* the PDT effect for bactericidal activity, but, more importantly, the sustained retention of the gel enables slow release of Ce6. This prolongs the photosensitizer's presence at the tumour site, thereby continuously recruiting macrophages and initiating an antitumour immune response, thereby significantly reducing the rate of postoperative recurrence. To address the challenge of poor penetration associated with topical drug administration, Chi *et al.*[230] proposed an enzyme-mediated nanocomposite hydrogel microneedle system (HAT@NP/TMPyP-MN). At the design level, the microneedles were engineered to physically breach the skin barrier. For controlled loading, TMPyP was first encapsulated

within PLGA nanoparticles, which were then embedded into an enzymatically crosslinked hyaluronic acid matrix. By modulating the crosslink density, the researchers achieved an ideal drug-release profile. Microneedles with medium crosslinking density exhibited optimal release kinetics, ensuring both a high loading capacity and sustained intratumoral retention. This release behaviour aligns precisely with the multiple light exposure windows required for PDT, thereby substantially enhancing the efficacy of transdermal PDT (Fig. 10j–l).

The limitations of monotherapy drive the combined use of PTT and PDT. To achieve synergistic effects in both time and space with therapeutic agents that have distinct mechanisms of action, the Zhu and Wang team[231] designed a delivery system based on dynamic chemistry. In this system, amide-functionalized carbon dots (NCD) serve as both the photo-therapeutic agent and the crosslinker. They form a dynamically crosslinked hydrogel with aldehyde-modified cellulose nanocrystals through Schiff base reactions. This design elegantly addresses the issue of leakage commonly associated with physical doping by chemically bonding the hydrophobic photo-therapeutic agents into the gel network, ensuring stable loading. In terms of release behaviour, the system undergoes rapid gelation within ten seconds. Upon laser irradiation, it simultaneously exerts photothermal and photodynamic effects. The resulting hyperthermia enhances tumour cells' sensitivity to ROS, resulting in a synergistic effect greater than the sum of its parts in combating melanoma.

6.4. Hydrogel-based delivery of immune modulators for melanoma therapy

Immunomodulators face substantial hurdles in systemic delivery, including short half-lives, poor tumour tissue accumulation, and the risk of systemic immune toxicity. Hydrogel-based local delivery platforms offer a rational design strategy for the programmed release of immune agonists and inhibitors. This approach can amplify antitumour immunity while minimising off-target effects.[232,233] Conventional immunotherapeutic approaches include high-dose interferon-α therapy, adoptive cell transfer, and biochemotherapy.[234,235] Advances in tumour immunology have broadened the therapeutic applications of immunotherapy, primarily through agents targeting immune checkpoints such as PD-1 and CTLA-4 antagonists.[236,237]

To address the challenge of maintaining therapeutic concentrations of immune checkpoint antibodies within the tumour microenvironment while limiting their systemic exposure, Kim *et al.*[238] In this design, the system remains liquid at 4 °C to facilitate injection and rapidly transitions into a gel state at body temperature, thereby forming a local drug depot. In terms of drug loading, this platform co-loads a hydrophobic NO donor (GSNO) and a hydrophilic antibody through physical encapsulation within the three-dimensional network of the gel. Release studies showed that the system enables slow, sustained drug release, thereby preventing rapid diffusion of antibodies in solution. This release profile ensures long-term retention of immunomodulators in the peritumoral region. Functionally, it not only prolongs immune stimulation but also enhances anti-melanoma efficacy through the synergistic action of continuously released NO and αCTLA-4. To improve the targeted delivery of the immunoadjuvant CpG to lymphoid tissues, the team further optimised the same platform. In terms of design,[239] the hydrogel's sustained release properties enabled a single peritumoral injection to achieve a pulse maintenance release pattern of CpG. The key to this release behaviour is that the hydrogel not only increased the total amount of CpG retained at the injection site, but more importantly, it extended the duration of its delivery to the tumour-draining lymph nodes. In terms of enhanced efficacy, this sustained delivery strategy significantly increased the enrichment and retention time of CpG in the TdLNs, thereby achieving more durable and potent dendritic cell maturation and T cell priming. This demonstrates that the location and intensity of immune activation can be precisely controlled by modulating the release kinetics.

In the postoperative setting, Yang *et al.*[240] designed a multifunctional hydrogel dressing (GelMA-CJCNPs) based on GelMA, incorporating carrier-free ternary nanoparticles (CJCNPs) loaded with the photosensitizer Ce6, BRD4 inhibitor JQ1, and glutaminase inhibitor C968 (Fig. 11a–d). This integrated platform's enhanced therapeutic effect is attributed to three key mechanisms. First, the hydrogel acts as a physical barrier that covers the postsurgical wound, helping prevent infection. Second, upon NIR light irradiation, Ce6 mediates PDT to induce local ICD. Third, the controlled release of JQ1 and C968 from the hydrogel persistently modulates the tumour microenvironment, suppressing the proliferation and metabolic activity of residual cancer cells. Therefore, this integrated design and delivery strategy achieves spatiotemporal synergy among local treatment, immune activation, and wound healing.

Furthermore, the emerging field of metallo-immunology inspires new strategies for hydrogel design. Zhu *et al.*[241] developed an adaptive dynamic hydrogel (VPHCh) using carboxymethyl chitosan as the matrix and incorporating vanadium-dopamine nanoparticles (V-PDA) with dual photothermal and catalytic activity. Upon NIR irradiation, the photothermal effect induced local hyperthermia, thereby simultaneously triggering the release of V^{5+} from the nanoparticles. The photothermal effect directly ablates tumour cells, while the sustained release of vanadium ions generates excess ROS *in situ*. This triggers ferroptosis in cancer cells, further amplifying ICD. This multimode synergy, derived from the material's design, effectively prevents melanoma recurrence after surgery and accelerates wound healing through chitosan's inherent properties.

6.5. Hydrogel-enhanced chemodynamic therapy for melanoma treatment

Chemodynamic therapy (CDT) has emerged as a tumour-selective therapeutic modality that exploits endogenous H_2O_2 within the TME to generate highly cytotoxic ROS, particularly hydroxyl radicals ($^{\bullet}OH$), *via* Fenton or Fenton-like reactions. This oxidative stress induces irreversible damage to lipids, proteins, and DNA, leading to tumour cell apoptosis and growth inhibition.[242] A major challenge in CDT is the high concentration of GSH in the TME, which scavenges $^{\bullet}OH$ and thereby

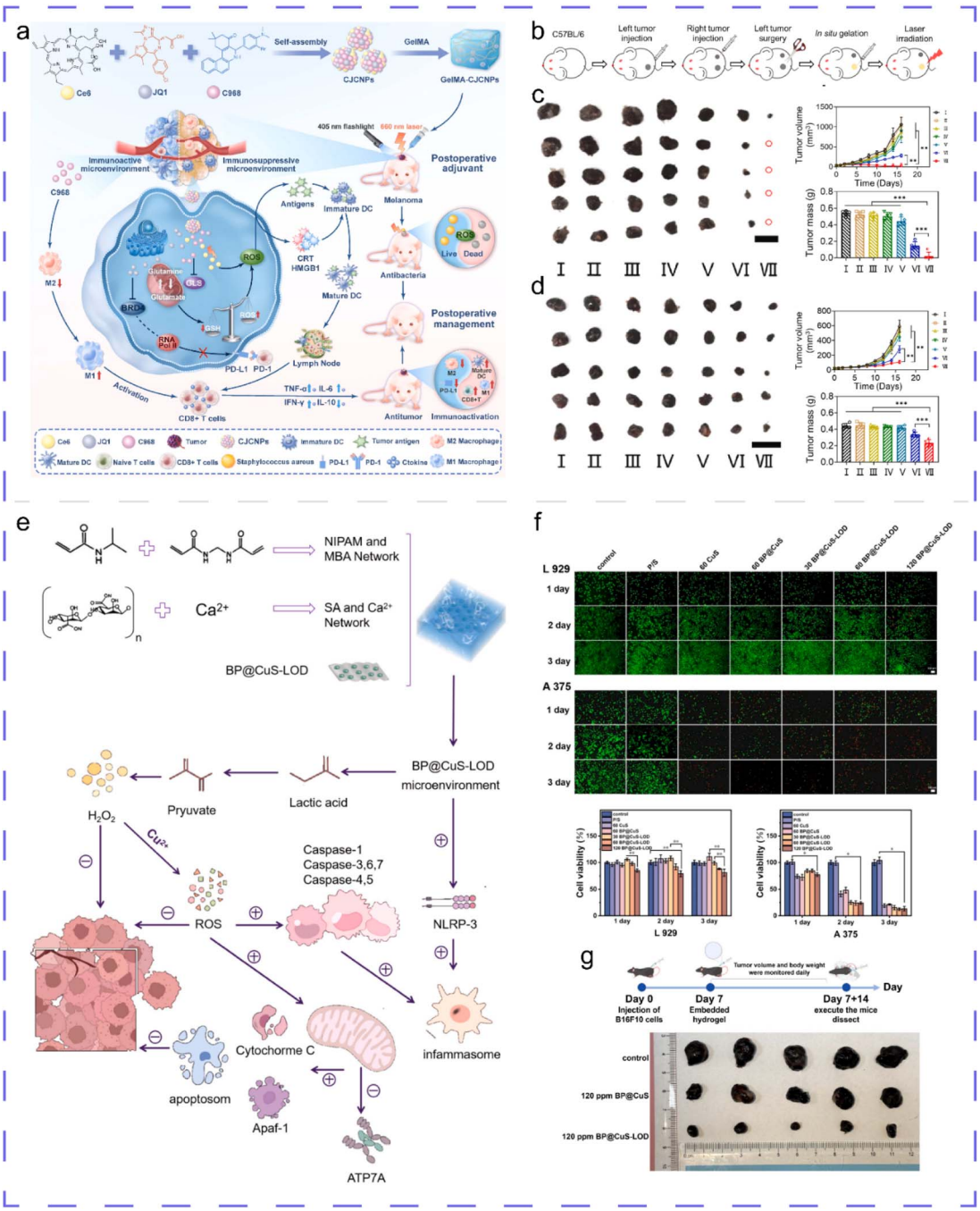

Fig. 11 (a) Schematic illustration of the immunotherapeutic hydrogel booster (GelMA-CJCNPs) for inhibiting postoperative tumour recurrence and promoting wound healing. (b) The bilateral tumour-bearing model was established by sequential injection of B16F10 cells. (c) *In vivo* anti-primary-tumour efficacy of GelMA-CJCNPs hydrogel in B16F10 melanoma-bearing mice. (d) *In vivo* anti-metastatic efficacy of GelMA-CJCNPs hydrogel in B16F10 melanoma-bearing mice. Adapted with permission from ref. 240, Copyright 2024, KeAi Communications Co. (e) Schematic illustration of the preparation and therapeutic mechanism of BP@CuS-LOD/PNIPAm/SA hydrogel. (f) BP@CuS-LOD hydrogel co-cultured with L929 and A375 cells for 1, 2, and 3 days: Live/dead staining and CCK-8 cell viability assay results. (g) Tumour suppression by BP@CuS-LOD hydrogel was evaluated in B16F10 tumour-bearing mice. Adapted with permission from ref. 247, Copyright 2026, Elsevier.

diminishes therapeutic efficacy. Copper ions (Cu^{2+}) offer a dual-functional solution to this limitation: first, Cu^{2+} oxidises GSH to GSSG, effectively depleting this antioxidant and alleviating its inhibitory effect on ROS accumulation; second, the resulting Cu^{+} can react with endogenous H_2O_2 through a Cu^{+}/Cu^{2+} redox cycle, driving sustained $^{\cdot}OH$ generation *via* a copper-mediated Fenton-like reaction, thus amplifying tumour cell killing.[243,244] In this context, hydrogel-based delivery systems play a pivotal role by enabling localised and prolonged retention of catalytic agents at tumour sites, facilitating targeted enrichment and

controlled release of functional nanomaterials. This spatiotemporally regulated delivery significantly improves the specificity and potency of CDT while minimising off-target effects, overcoming key limitations of conventional systemic administration.[245,246]

Recent advances have demonstrated diverse strategies for enhancing CDT efficacy through rational hydrogel design that integrates carrier properties with therapeutic mechanisms, following a clear design-load-release-efficacy paradigm. From the perspective of optimising catalytic efficiency, the design by Chen *et al.*[247] exemplifies a strategy for adapting and loading multi-component therapeutics. They constructed a thermosensitive twin-network hydrogel, specifically a NIPAm/SA interpenetrating polymer network (Fig. 11e–g). In this system, the hydrophilic network provides a mild encapsulation environment for lactate oxidase (LOD), thereby preserving its bioactivity. Meanwhile, the hydrophobic microdomains or interstitial spaces within the network physically accommodate black phosphorus copper sulfide nanoparticles (BP@CuS). This design capitalises on the high lactate levels in the tumour microenvironment (TME) to trigger *in situ* release and catalytic activity. After the hydrogel forms at the tumour site, lactate oxidase (LOD) first catalyses the oxidation of lactate to produce H_2O_2. This reaction then activates a Cu^{2+}-mediated Fenton-like reaction within the gel, generating highly toxic hydroxyl radicals ($^{\bullet}OH$). Concurrently, external NIR irradiation triggers the photothermal effect of BP@CuS. This thermal effect not only accelerates mass transfer and ROS diffusion within the gel but also enhances tumour penetration and cytotoxicity through mild hyperthermia. The result is photothermal-enhanced CDT and Cu^{2+} overload-induced pyroptosis. Through this controlled, multi-stage generation and release of ROS, the system effectively inhibits melanoma growth and metastasis *in vitro* and *in vivo*.

Starting from molecular design, Pi *et al.*[248] engineered an injectable ternary hydrogel (GA-Cu^{2+}-NCTD) composed of GA, Cu^{2+} and norcantharidin. Within this system, Cu^{2+} functions as both a critical crosslinking centre and a catalyst for CDT. It is precisely coordinated within the glycyrrhizic acid hydrogel network. Upon injection, the system responds to the weakly acidic tumour microenvironment (TME) by gradually dissociating, releasing Cu^{2+} and NCTD. The released Cu^{2+} then generates ROS *in situ* through a photo-Fenton-like reaction. This action synergises with NCTD-induced apoptosis and cuproptosis to achieve potent antitumour effects. Zhang *et al.*[249] constructed an SA-MPS hydrogel by embedding $MnPSe_3$ nanosheets into a sodium alginate matrix. The Mn^{2+}/Mn^{3+} redox pairs exhibit intrinsic Fenton-like activity, allowing autonomous conversion of residual H_2O_2 into $^{\bullet}OH$ in the postoperative tumour bed without external stimuli. This sustained and localised release of ROS, which requires no external energy input, aligns precisely with the therapeutic window for eliminating residual tumour cells in the postoperative microenvironment. The results showed that a single application of the SA-MPS hydrogel inhibited the activity of 56.2% of residual tumour cells, significantly lowering the risk of postoperative recurrence.

In summary, these systems leverage sophisticated hydrogel engineering to precisely control the loading and activation of metal ion catalysts, such as Cu^{2+} and Mn^{2+}. This design enables the sustained conversion of endogenous tumour H_2O_2. Into highly toxic $^{\bullet}OH$, creating a logical and effective bridge between material design and therapeutic outcome. Consequently, these platforms demonstrate substantial potential for treating primary melanoma, preventing postoperative recurrence, and inhibiting distant metastasis.

7. Clinical translation prospects and challenges

Cancer profoundly affects patients' physical and mental health and significantly diminishes their quality of life, making effective treatment a critical unmet need in clinical practice. Hydrogel-based melanoma delivery systems offer considerable clinical potential due to their ability to enable controlled drug release, excellent biocompatibility, and responsiveness to the TME. Regulatory authorities, including the FDA and the European Commission, have recognised key components commonly used to construct such hydrogels as safe materials.[250] These components include PEG, gelatin, and HA. Furthermore, clinically approved hydrogel-based products, such as dermal fillers and wound dressings, have already entered the market[251,252] providing a strong translational foundation for developing hydrogel-based melanoma therapies and reducing regulatory barriers. Despite these advantages, significant challenges remain in translating hydrogel delivery systems into routine clinical use. First, the complexity and dynamic nature of human physiological and biochemical environments limit the clinical relevance of current research, much of which remains confined to *in vitro* studies. Long-term *in vivo* data on safety and efficacy are still insufficient. Certain synthetic hydrogels, such as chemically cross-linked polyacrylamide-based formulations, pose specific concerns. These include potential residual toxicity from precursor materials and the risk of inflammatory responses triggered by their degradation by-products. Moreover, once implanted, hydrogels can be recognised as foreign bodies by the immune system, eliciting chronic inflammatory responses that impair integration with host tissues. Some formulations also degrade too slowly, increasing the risk of persistent foreign body reactions. Second, achieving precise spatiotemporal control over drug release remains a major hurdle. Conventional hydrogels within the target tumour region. This leads to inconsistent therapeutic outcomes and increases the risk of systemic toxicity, often diverging from intended treatment goals. Although smart hydrogels have been developed, most rely on single-stimuli responsiveness, whereas the *in vivo* environment involves multiple interdependent physiological cues. As a result, single-mode systems often fail to achieve accurate, context-specific activation. Additionally, there is an inherent trade-off between sensitivity and stability: highly responsive hydrogels may release drugs prematurely due to off-target stimuli, while overly stable systems exhibit delayed responses, failing to meet real-time pathological demands.

Third, challenges in scalable manufacturing and batch-to-batch consistency hinder clinical translation. Laboratory-scale hydrogel fabrication typically involves small volumes and manual, labour-intensive processes that are difficult to scale up for industrial production. During scale-up, issues such as non-uniform crosslinking, variable pore size distribution, and inconsistent mechanical properties commonly arise, leading to significant variability between batches and compromising product reliability.

In response to the aforementioned challenges, future research should focus on strategic advancements across multiple fronts. First, advanced technologies such as 3D bioprinting and microfluidic chips can be leveraged to develop *in vitro* models that accurately recapitulate the melanoma TME, thereby bridging the gap between *in vitro* findings and *in vivo* outcomes. Stepwise *in vivo* validation, progressing from small to large animal models, should be systematically conducted to generate robust long-term safety and efficacy data. Preclinical pharmacokinetic and pharmacodynamic (PK/PD) evaluations are essential to inform rational clinical dosing regimens. To mitigate toxicity risks associated with synthetic hydrogels, priority should be given to natural, biodegradable materials, and physical cross-linking strategies driven by hydrogen bonding or hydrophobic interactions should replace conventional chemical cross-linking methods, minimising reliance on potentially harmful polymers such as polyacrylamide. Rigorous purification protocols must be implemented to reduce residual monomers, and formulations should be designed so that degradation byproducts are low-molecular-weight metabolites readily cleared by physiological pathways. Improving *in vivo* immunocompatibility is critical: surface functionalization with bioactive moieties, such as RGD peptides or immune-modulating agents, can reduce immune recognition of the hydrogel as a foreign body and enhance its integration with host tissues. When indicated, localised delivery of anti-inflammatory agents *via* sustained release can further suppress chronic inflammatory responses. The degradation kinetics of hydrogels should be precisely tuned by modulating cross-linker concentration, reaction duration, or incorporating enzyme-sensitive or pH-responsive dynamic bonds to align with the temporal demands of tumour therapy, thereby preventing persistent foreign body reactions due to excessively slow degradation. Second, to achieve precise drug release control, multi-layered or core–shell hydrogel architectures can be engineered to enable multi-stimuli responsiveness. These structures can serve as physical barriers to prevent initial burst release and facilitate sustained, controlled drug elution. Integration of miniature optical fibre sensors or fluorescent probes into the hydrogel matrix enables real-time monitoring of local drug concentrations at the lesion site. Coupled with molecular-to-mesoscopic-scale simulations and advanced imaging techniques, this allows detailed mapping of non-covalent and covalent interactions between the carrier and the drug payload, enabling the reverse engineering of release kinetics for spatiotemporally precise delivery. For intelligent responsive systems, overcoming the limitations of single-stimulus activation requires the development of multi-signal cooperative hydrogels that integrate key pathological cues from the melanoma microenvironment. Logic-gated release mechanisms triggered by multiple concurrent stimuli can significantly improve targeting specificity and accuracy. Furthermore, sensor-informed feedback loops can guide external, non-invasive stimuli such as NIR irradiation or magnetic fields to dynamically modulate drug release, minimising systemic exposure and associated toxicities. To balance sensitivity and stability, hybrid cross-linking networks combining dynamic covalent bonds (*e.g.*, Schiff bases, disulfide bonds) with reversible non-covalent interactions (*e.g.*, hydrogen bonding, hydrophobic assembly) can be employed. This dual-network design confers rapid responsiveness to target stimuli while maintaining structural integrity under off-target conditions, thereby reducing false triggers and enhancing overall system reliability. Finally, scalable and reproducible manufacturing is paramount for clinical translation. Standardised operating procedures for critical process parameters must be established, supported by real-time online monitoring to ensure batch-to-batch consistency. Variability in mechanical properties and pore architecture should be tightly controlled within predefined tolerances. Raw material sourcing must be standardised, and continuous production platforms, such as microfluidic systems, should replace traditional batch processes to enhance homogeneity and scalability, ultimately minimising inter-batch heterogeneity and supporting regulatory compliance.

8. Conclusions and perspectives

Hydrogels have emerged as an advanced delivery platform for local treatment of CM, owing to their biodegradability, biocompatibility, and chemically tunable functionality enabled by diverse polymer compositions and crosslinking strategies. This platform can be flexibly loaded with various therapeutic agents, enabling sustained drug release at the tumour site and effectively overcoming the limitations of conventional therapies. This Review systematically examines hydrogel-based delivery systems for the treatment of CM. It explores the network structures generated by different crosslinking strategies, including physical, chemical, and dual-crosslinking methods. The discussion focuses on how these structures relate to drug loading capacity, release kinetics, and responsiveness to the tumour microenvironment. However, several critical hurdles must be addressed to advance their clinical translation. At the material level, it is necessary to balance the controllability of synthetic polymers with the biosafety of natural polymers, while also resolving quality control issues arising from significant batch-to-batch variability in natural sources. At the process level, establishing gentle sterilisation methods that do not compromise gel structure or therapeutic efficacy, and defining the long-term storage stability of formulations, remain key challenges. At the mechanistic level, current research primarily focuses on treatment efficacy, but the structure–activity relationships governing hydrogel-tumour microenvironment interactions, as well as the mechanisms governing precise drug release, remain underexplored. Addressing these hurdles through rational design and advanced

characterisation will be crucial to bridging the gap between bench research and clinical practice, ultimately unlocking the full potential of hydrogel-based therapies.

Future efforts should focus on addressing these challenges. Advancing this field will require an interdisciplinary approach that integrates materials science with pharmaceutical and biological research. Key strategies include developing intelligent, responsive, or hybrid systems with precisely engineered chemical structures to optimise material properties, conducting in-depth investigations into structure–activity relationships *in vivo* to guide precision therapy, and establishing standardised protocols for sterilisation and storage. With continued multidisciplinary progress, functional hydrogels that integrate controlled release, sustained delivery, and efficient targeting are expected to emerge. Such innovations could establish a new, minimally invasive, and low-toxicity therapeutic paradigm for CM, ultimately benefiting patients.

Author contributions

Yunying Wu and Wei Zheng: conceptualisation, investigation, writing—original draft preparation; Xiao Li: review and editing; Shengguang Wu: resources and review; Liangliang Zhou: supervision, writing—review and editing; Ding Zhang: project administration, supervision, writing—review and editing; Zhenhua Chen: writing—review and editing, supervision. All authors have read and agreed to the published version of the manuscript.

Conflicts of interest

There are no conflicts to declare.

Data availability

No primary research results, software or code have been included, and no new data were generated or analysed as part of this review.

Acknowledgements

This work was financially supported by the Outstanding Young Talents Funding of Jiangxi Province (grant no. 20224ACB216019), Science and Technology Research Project of Jiangxi Provincial Department of Education (grant no. GJJ2501207), the PhD Start-up Fund of Science Research Project of Jiangxi Science and Technology Normal University (grant no. 2024BSQD114).

References

1 F. Alenezi, A. Armghan and K. Polat, *Diagnostics*, 2023, **13**, 262.
2 C. Di Raimondo, F. Lozzi, P. P. Di Domenico, E. Campione and L. Bianchi, *Int. J. Mol. Sci.*, 2023, **24**, 14535.
3 R. L. Siegel, T. B. Kratzer, A. N. Giaquinto, H. Sung and A. Jemal, *Ca*, 2025, **75**, 10.
4 S. Waseh and J. B. Lee, *Front. Med.*, 2023, **10**, 1268479.
5 M. Arnold, D. Singh, M. Laversanne, J. Vignat, S. Vaccarella, F. Meheus, A. E. Cust, E. De Vries, D. C. Whiteman and F. Bray, *JAMA Dermatol.*, 2022, **158**, 495–503.
6 Y. Sun, Y. Shen, Q. Liu, H. Zhang, L. Jia, Y. Chai, H. Jiang, M. Wu and Y. Li, *J. Am. Acad. Dermatol.*, 2025, **92**, 100–107.
7 J. Lopes, C. M. Rodrigues, M. M. Gaspar and C. P. Reis, *Cancers*, 2022, **14**, 4652.
8 N. Hasan, A. Nadaf, M. Imran, U. Jiba, A. Sheikh, W. H. Almalki, S. S. Almujri, Y. H. Mohammed, P. Kesharwani and F. J. Ahmad, *Mol. Cancer*, 2023, **22**, 168.
9 M. Donia, H. Jespersen, M. Jalving, R. Lee, H. Eriksson, C. Hoeller, M. Hernberg, I. Gavrilova, L. Kandolf and G. Liszkay, *ESMO Open*, 2025, **10**, 104295.
10 J. L. Liang, G. F. Luo, W. H. Chen and X. Z. Zhang, *Adv. Mater.*, 2021, **33**, 2007630.
11 Y. Cai, T. Chai, W. Nguyen, J. Liu, E. Xiao, X. Ran, Y. Ran, D. Du, W. Chen and X. Chen, *Signal Transduct. Targeted Ther.*, 2025, **10**, 115.
12 S. S. Moni, J. M. Moshi, S. Matou-Nasri, S. Alotaibi, Y. M. Hawsawi, M. E. Elmobark, A. M. S. Hakami, M. A. Jeraiby, A. A. Sulayli and H. N. Moafa, *Pharmaceutics*, 2025, **17**, 296.
13 M. M. El Sayed, *J. Polym. Environ.*, 2023, **31**, 2855–2879.
14 M. A. Badsha, M. Khan, B. Wu, A. Kumar and I. M. Lo, *J. Hazard Mater.*, 2021, **408**, 124463.
15 M. M. Bhuyan and J.-H. Jeong, *Gels*, 2025, **11**, 896.
16 H. Huang, X. Wang, W. Wang, X. Qu, X. Song, Y. Zhang, L. Zhong, D.-p. Yang, X. Dong and Y. Zhao, *Biomaterials*, 2022, **280**, 121289.
17 Z. Zhang, Z. Zhang, W. Zeng, Y. Li and C. Zhu, *Int. J. Biol. Macromol.*, 2024, **283**, 138039.
18 W. Wang, X. Ma, W. Gu, H. Xu, Z. Zhang, H. Dai, H. Wu and H. Lv, *Int. J. Biol. Macromol.*, 2024, **281**, 136397.
19 Q. Chen, C. Wang, X. Zhang, G. Chen, Q. Hu, H. Li, J. Wang, D. Wen, Y. Zhang and Y. Lu, *Nat. Nanotechnol.*, 2019, **14**, 89–97.
20 Q. Hu, H. Li, E. Archibong, Q. Chen, H. Ruan, S. Ahn, E. Dukhovlinova, Y. Kang, D. Wen and G. Dotti, *Nat. Biomed. Eng.*, 2021, **5**, 1038–1047.
21 P. P. Centeno, V. Pavet and R. Marais, *Nat. Rev. Cancer*, 2023, **23**, 372–390.
22 L. M. Gosman, D.-A. Tăpoi and M. Costache, *Int. J. Mol. Sci.*, 2023, **24**, 15881.
23 N. L. Bolick and A. C. Geller, *Hematol./Oncol. Clin.*, 2021, **35**, 57–72.
24 A. A. Chan, J. Noguti, N. M. Ramirez, M. Navarrete and D. J. Lee, *J. Invest. Dermatol.*, 2026, **146**, 771–781.
25 A. Barreiro-Capurro, J. J. Andres-Lencina, S. Podlipnik, C. Carrera, C. Requena, E. Manrique-Silva, P. Quaglino, L. Tonella, A. Jaka and N. Richarz, *Eur. J. Cancer*, 2021, **145**, 29–37.
26 J. E. Gershenwald and R. A. Scolyer, *Ann. Surg Oncol.*, 2018, **25**, 2105–2110.
27 H. J. Kim and Y. H. Kim, *Int. J. Mol. Sci.*, 2024, **25**, 2984.

28 R. M. Slominski, T. Sarna, P. M. Płonka, C. Raman, A. A. Brożyna and A. T. Slominski, *Front. Oncol.*, 2022, **12**, 842496.
29 W. Saeed, E. Shahbaz, Q. Maqsood, S. W. Ali and M. Mahnoor, *Cancer Control*, 2024, **31**, 10732748241274978.
30 S. Song, F. Li, B. Zhao, M. Zhou and X. Wang, *Adv. Biol.*, 2025, **9**, 2400090.
31 O. Langselius, H. Rumgay, E. de Vries, D. C. Whiteman, A. Jemal, D. M. Parkin and I. Soerjomataram, *Int. J. Cancer*, 2025, **157**, 1110–1119.
32 H. Xu, S. Ren, Y. Wang, T. Zhang and J. Lu, *Cancer Adv.*, 2025, **8**, e25002.
33 L. Zhao, Y. Zhou, J. Zhang, H. Liang, X. Chen and H. Tan, *Pharmaceutics*, 2023, **15**, 2514.
34 M. Sobczak, *Int. J. Mol. Sci.*, 2022, **23**, 4421.
35 Y. Liu, L. Si, Y. Jiang, S. Jiang, X. Zhang, S. Li, J. Chen and J. Hu, *Int. J. Nanomed.*, 2025, 705–721.
36 A. Zhang, K. Miao, H. Sun and C.-X. Deng, *Int. J. Biol. Sci.*, 2022, **18**, 3019.
37 U. S. Madduma-Bandarage and S. V. Madihally, *J. Appl. Polym. Sci.*, 2021, **138**, 50376.
38 Z. Ahmad, S. Salman, S. A. Khan, A. Amin, Z. U. Rahman, Y. O. Al-Ghamdi, K. Akhtar, E. M. Bakhsh and S. B. Khan, *Gels*, 2022, **8**, 167.
39 P. Haddow, W. McAuley, S. Kirton and M. T. Cook, *Mater. Adv.*, 2020, **1**, 371–386.
40 Z. Nikfarjam and N. Biglari, *Nano Micro Biosyst.*, 2025, **4**, 45–51.
41 J. Zhang, J. Liu, A. Liu, S. He and W. Shao, *Sens. Actuators, B*, 2023, **390**, 133899.
42 R. Yang, C. Xia, C. Mei and J. Li, *J. Bioresour. Bioprod.*, 2025, **10**, 145–169.
43 U. Hwang, H. Moon, J. Park and H. W. Jung, *Polymers*, 2024, **16**, 2149.
44 Y. Naguib, F. M. Mady and K. A. Khaled, *J. Adv. Biomedical Pharm. Sci.*, 2024, **7**, 26–36.
45 G. J. Rodriguez-Rivera, M. Green, V. Shah, K. Leyendecker and E. Cosgriff-Hernandez, *J. Biomed. Mater. Res., Part A*, 2024, **112**, 1200–1212.
46 Z. Wang, Q. Ye, S. Yu and B. Akhavan, *Adv. Healthcare Mater.*, 2023, **12**, 2300105.
47 A.-E. Segneanu, L. E. Bejenaru, C. Bejenaru, A. Blendea, G. D. Mogoșanu, A. Biță and E. R. Boia, *Polymers*, 2025, **17**, 2026.
48 S. Khattak, I. Ullah, M. T. Yousaf, S. Ullah, H. Yousaf, Y. Li, H. Jin, J. Shen and H.-T. Xu, *Int. J. Biol. Macromol.*, 2025, **327**, 147270.
49 C. Vasile, D. Pamfil, E. Stoleru and M. Baican, *Molecules*, 2020, **25**, 1539.
50 C. Mortier, D. Costa, M. B. Oliveira, H. J. Haugen, S. P. Lyngstadaas, J. Blaker and J. Mano, *Mater. Today Chem.*, 2022, **26**, 101222.
51 R. Gharios, R. M. Francis and C. A. DeForest, *Matter*, 2023, **6**, 4195–4244.
52 S. B. Bhalerao, V. R. Mahajan and R. R. Maske, *World J. Biol. Pharm. Health Sci.*, 2022, **12**, 39–53.
53 T. Shen, Y. Zhang, L. Mei, X.-B. Zhang and G. Zhu, *Theranostics*, 2022, **12**, 35.
54 H. Zhao, L. Wang, S. Yang, Z. Li, X. Guo, C. Zuo, G. Xie, C. Yao and D. Yang, *J. Am. Chem. Soc.*, 2025, **147**, 21194–21208.
55 H. N. Abdelhamid and A. P. Mathew, *Int. J. Mol. Sci.*, 2022, **23**, 5405.
56 A. Jafari, A. Al-Ostaz and S. Nouranian, *Polym. Adv. Technol.*, 2024, **35**, e6621.
57 N. Zhong, N. Cao, Z. Cheng, S. Fang, M. Jiang, J. Guan, W. Wang and X. Zang, *ACS Appl. Bio Mater.*, 2025, **8**, 5532–5546.
58 E. Meco and K. J. Lampe, *Biomacromolecules*, 2019, **20**, 1914–1925.
59 Z. Guo, Y. Xu, L. Dong, M. S. Desai, J. Xia, M. Liang, S.-W. Lee, S. Mi and W. Sun, *Chem. Eng. J.*, 2022, **435**, 135155.
60 N. Asadi, A. Mehdipour, M. Ghorbani, M. Mesgari-Abbasi, A. Akbarzadeh and S. Davaran, *Int. J. Biol. Macromol.*, 2021, **193**, 734–747.
61 Y. Lu, W. Kang, Y. Yu, H. Lu, Y. Wang, Z. Xu, J. Zeng, M. Qin and X. Xu, *Int. J. Biol. Macromol.*, 2024, **269**, 131795.
62 C. G. Cisneros, H. Agten, E. Derveaux, P. Adriaensens, V. Bloemen and A. Mignon, *React. Funct. Polym.*, 2025, 106330.
63 Y. Liang, B. Chen, M. Li, J. He, Z. Yin and B. Guo, *Biomacromolecules*, 2020, **21**, 1841–1852.
64 V. Sousa, L. P. Monteiro, D. H. Rocha, J. M. Rodrigues, J. Borges and J. F. Mano, *Biomacromolecules*, 2025, **26**, 4735–4772.
65 V. G. Muir and J. A. Burdick, *Chem. Rev.*, 2020, **121**, 10908–10949.
66 M. Muhammad, C. Willems, J. Rodríguez-Fernández, G. Gallego-Ferrer and T. Groth, *Biomolecules*, 2020, **10**, 1185.
67 C. O. Pandeirada, D. W. Merkx, H.-G. Janssen, Y. Westphal and H. A. Schols, *Carbohydr. Polym.*, 2021, **259**, 117781.
68 W. Ding, Y.-n. Wang, J. Zhou and B. Shi, *Carbohydr. Polym.*, 2018, **201**, 549–556.
69 C. Mo, L. Xiang and Y. Chen, *Macromol. Rapid Commun.*, 2021, **42**, 2100025.
70 K. Sahajpal, S. Shekhar, A. Kumar, B. Sharma, M. K. Meena, A. K. Bhagi and S. Sharma, *J. Mater. Chem. B*, 2022, **10**, 3173–3198.
71 R. Li, Y. Wu, L. He, R. Yang, K. Luo, F. Gao, H. Yuan, Y. Zheng and Y. He, *Mater. Des.*, 2025, 114128.
72 X. Liu, J. Hu, Y. Hu, Y. Liu, Y. Wei and D. Huang, *Colloids Surf., B*, 2025, **245**, 114346.
73 R. Li, Y. Zhao, S. Zhang, Y. Liu, C. Chi, D. Wu and J. Song, *Macromol. Biosci.*, 2025, e00084.
74 Y. Zhong, F. Seidi, Y. Wang, L. Zheng, Y. Jin and H. Xiao, *Carbohydr. Polym.*, 2022, **298**, 120103.
75 D. Xia, P. Wang, X. Ji, N. M. Khashab, J. L. Sessler and F. Huang, *Chem. Rev.*, 2020, **120**, 6070–6123.
76 S. Duan, M. Hua, C. W. Zhang, W. Hong, Y. Yan, A. Jazzar, C. Chen, P. Shi, M. Si and D. Wu, *Chem. Rev.*, 2025, **125**, 7918–7964.

77 Z. Li, F. Lu and Y. Liu, *J. Agric. Food Chem.*, 2023, **71**, 10238–10249.
78 M. J. Webber and M. W. Tibbitt, *Nat. Rev. Mater.*, 2022, **7**, 541–556.
79 Y. Huang, S. M. Morozova, T. Li, S. Li, H. E. Naguib and E. Kumacheva, *Biomacromolecules*, 2022, **24**, 1173–1183.
80 D. Zhang, Z. Li, L. Yang, H. Ma, H. Chen and X. Zeng, *Biomaterials*, 2023, **303**, 122388.
81 R. Foudazi, R. Zowada, I. Manas-Zloczower and D. L. Feke, *Langmuir*, 2023, **39**, 2092–2111.
82 J. L. Schiller and S. K. Lai, *ACS Appl. Bio Mater.*, 2020, **3**, 2875–2890.
83 E. C. de Siqueira, J. A. A. de França, R. F. M. de Souza, D. M. da Silva Leoterio, J. N. Cordeiro and B. Doboszewski, *Res. Soc. Dev.*, 2023, **12**, e18312943072.
84 A. Sharma, H. Chopra, I. Singh and T. B. Emran, *Int. J. Surg.*, 2022, **106**, 106915.
85 S. Dong, S. An, Q. Saiding, Q. Chen, B. Liu, N. Kong, W. Chen and W. Tao, *Chem. Rev.*, 2025, **125**, 8835–8920.
86 K. J. De France, F. Xu and T. Hoare, *Adv. Healthcare Mater.*, 2018, **7**, 1700927.
87 S. M. Morozova, A. Gevorkian and E. Kumacheva, *Chem. Soc. Rev.*, 2023, **52**, 5317–5339.
88 Y. Alsaid, S. Wu, D. Wu, Y. Du, L. Shi, R. Khodambashi, R. Rico, M. Hua, Y. Yan and Y. Zhao, *Adv. Mater.*, 2021, **33**, 2008235.
89 B. G. Amsden, *Macromolecules*, 2022, **55**, 8399–8408.
90 S. Ishikawa, Y. Iwanaga, T. Uneyama, X. Li, H. Hojo, I. Fujinaga, T. Katashima, T. Saito, Y. Okada and U.-i. Chung, *Nat. Mater.*, 2023, **22**, 1564–1570.
91 G. Aizik, C. A. Ostertag-Hill, P. Chakraborty, W. Choi, M. Pan, D. V. Mankus, A. K. Lytton-Jean and D. S. Kohane, *Acta Biomater.*, 2024, **183**, 101–110.
92 X. Zheng, X. Liu and L. Zha, *J. Appl. Polym. Sci.*, 2021, **138**, 50280.
93 W. Hu, Z. Wang, Y. Xiao, S. Zhang and J. Wang, *Biomater. Sci.*, 2019, **7**, 843–855.
94 A. Oryan, A. Kamali, A. Moshiri, H. Baharvand and H. Daemi, *Int. J. Biol. Macromol.*, 2018, **107**, 678–688.
95 P. Sapuła, K. Bialik-Wąs and K. Malarz, *Pharmaceutics*, 2023, **15**, 253.
96 C. Xiang, Z. Guo, Q. Zhang, Z. Wang, X. Li, W. Chen, X. Wei, P. Li and C. Xiang, *Mater. Des.*, 2024, **243**, 113048.
97 J. Cong, X. Liu, C. Li, L. Mei, S. Pan, J. Tian, T. Xu, C. Miao, W. Ding and T. Luo, *ACS Appl. Polym. Mater.*, 2025, **7**, 12321–12336.
98 Y. Xiong, T. Wang, L. Liu, Y. Kou, Z. Zhao, M. Yuan, Y. Chen, D. Wang and S. Song, *Chem. Eng. J.*, 2023, **451**, 138889.
99 L. Zhu, Q. Lu, T. Bian, P. Yang, Y. Yang and L. Zhang, *ACS Biomater. Sci. Eng.*, 2023, **9**, 4761–4769.
100 J. Xu, J. Li, X. Hu, D. Zhong, W. Chen and S. Qu, *J. Mech. Phys. Solid.*, 2024, **185**, 105571.
101 T. Zhang, Z. Liu, H. Aslan, C. Zhang and M. Yu, *J. Mater. Chem. B*, 2020, **8**, 6429–6437.
102 S. Ko, J. Y. Park and Y.-K. Oh, *Cancer Res.*, 2019, **79**, 6178–6189.
103 Y.-J. Jo, M. Gulfam, S.-H. Jo, Y.-S. Gal, C.-W. Oh, S.-H. Park and K. T. Lim, *Carbohydr. Polym.*, 2022, **286**, 119303.
104 C. Zhang, J. Ma, Q. Wang, Y. Wang, Z. Kang, Y. Chen, Z. Hui and X. Wang, *ACS Appl. Nano Mater.*, 2023, **6**, 7841–7854.
105 J.-H. Yang, W.-L. Du, H.-J. Tan, Y.-X. Zong, Q.-N. Wang, B.-S. Zhao, Z.-G. Wang, R. Zhang, J.-Z. Xu and Z.-M. Li, *J. Mater. Chem. B*, 2025, **13**, 8051–8058.
106 Z. Meng, X. Zhou, J. Xu, X. Han, Z. Dong, H. Wang, Y. Zhang, J. She, L. Xu and C. Wang, *Adv. Mater.*, 2019, **31**, 1900927.
107 Y. Zhang, S. Tian, L. Huang, Y. Li, Y. Lu, H. Li, G. Chen, F. Meng, G. L. Liu and X. Yang, *Nat. Commun.*, 2022, **13**, 4553.
108 Y. Guo, B. Tian, Y. Xie and J. Xiao, *J. Mater. Chem. B*, 2025, **13**, 12938–12948.
109 B. Zhu, Y. Cai, L. Zhou, L. Zhao, J. Chen, X. Shan, X. Sun, Q. You, X. Gong and W. Zhang, *Nat. Commun.*, 2025, **16**, 687.
110 C. Wu, J. Liu, Z. Zhai, L. Yang, X. Tang, L. Zhao, K. Xu and W. Zhong, *Acta Biomater.*, 2020, **106**, 278–288.
111 W. Fang, L. Yang, Y. Chen and Q. Hu, *Acta Biomater.*, 2023, **161**, 50–66.
112 W. Chu, M. Nie, X. Ke, J. Luo and J. Li, *Macromol. Biosci.*, 2021, **21**, 2100109.
113 Y. Ye, W. Wang, X. Liu, Y. Chen, S. Tian and P. Fu, *Gels*, 2023, **10**, 21.
114 Z. Wang, B. Zhai, J. Sun, X. Zhang, J. Zou, Y. Shi and D. Guo, *Drug Deliv.*, 2024, **31**, 2400476.
115 L. Zhu, G. Qiao, H. Gao, A. Jiang, L. Zhang and X. Wang, *Front. Oncol.*, 2025, **15**, 1590534.
116 M. Slavkova, B. Tzankov, T. Popova and C. Voycheva, *Gels*, 2023, **9**, 352.
117 K. Kathe and H. Kathpalia, *Asian J. Pharm. Sci.*, 2017, **12**, 487–497.
118 S. Bera, H. K. Datta and P. Dastidar, *Biomater. Sci.*, 2023, **11**, 5618–5633.
119 S. Hochheim, A. F. da Cruz, L. M. Zimmermann, L. L. Del Mercato, C. C. de Oliveira and I. C. Riegel-Vidotti, *Int. J. Biol. Macromol.*, 2025, 147958.
120 P. Liu, L. Hao, J. C. Hsu, M. Zhou, Z. Luo, Y. Peng, W. Cai and S. Hu, *Adv. Sci.*, 2025, **12**, 2414468.
121 Y. Wu, Y. Xiao, B. Yin and S. H. D. Wong, *Int. J. Mol. Sci.*, 2025, **26**, 9502.
122 W. Yang, J. Chen, Z. Zhao, M. Wu, L. Gong, Y. Sun, C. Huang, B. Yan and H. Zeng, *J. Mater. Chem. B*, 2024, **12**, 332–349.
123 J. Liu, C. Du, W. Huang and Y. Lei, *Biomater. Sci.*, 2024, **12**, 8–56.
124 A. Roy, K. Manna and S. Pal, *Mater. Chem. Front.*, 2022, **6**, 2338–2385.
125 P. Bertsch, M. Diba, D. J. Mooney and S. C. Leeuwenburgh, *Chem. Rev.*, 2022, **123**, 834–873.
126 S. Kim, D.-D. Kim, M. Karmakar and H.-J. Cho, *J. Pharm. Investig.*, 2024, **54**, 555–591.
127 G. Alotaibi, S. Alharthi, B. Basu, D. Ash, S. Dutta, S. Singh, B. G. Prajapati, S. Bhattacharya, V. R. Chidrawar and H. Chitme, *Gels*, 2023, **9**, 331.

128 P. Sahu, S. K. Kashaw, S. Sau, V. Kushwah, S. Jain, R. K. Agrawal and A. K. Iyer, *Colloids Surf., B*, 2019, **174**, 232–245.
129 Q. Lv, C. He, F. Quan, S. Yu and X. Chen, *Bioact. Mater.*, 2018, **3**, 118–128.
130 A. Vashist, V. Atluri, A. Raymond, A. Kaushik, T. Parira, Z. Huang, A. Durygin, A. Tomitaka, R. Nikkhah-Moshaie and A. Vashist, *Front. Bioeng. Biotechnol.*, 2020, **8**, 315.
131 N. Bharti, V. Kumar, S. Mukherjee, D. Das, S. Das, D. Kashyap, S. Shafi, S. Srivastava, M. K. Mishra and A. K. Singh, *Pharm. Dev. Technol.*, 2025, **30**, 1449–1475.
132 X. Wang, Z. Wang, M. Xiao, Z. Li and Z. Zhu, *Biomater. Sci.*, 2024, **12**, 530–563.
133 D. Ando, M. Miyatsuji, H. Sakoda, E. Yamamoto, T. Miyazaki, T. Koide, Y. Sato and K.-i. Izutsu, *Pharmaceutics*, 2024, **16**, 200.
134 S. Bhatnagar, P. R. Gadeela, P. Thathireddy and V. V. K. Venuganti, *J. Chem. Sci.*, 2019, **131**, 90.
135 N. Huang, K. J. Lee and M. S. Stark, *Front. Med.*, 2022, **9**, 873728.
136 B. Zhuang, T. Chen, Z. Xiao and Y. Jin, *Int. J. Pharm.*, 2020, **577**, 119048.
137 C. T. Hagan IV, C. Bloomquist, S. Warner, N. M. Knape, I. Kim, H. Foley, K. T. Wagner, S. Mecham, J. DeSimone and A. Z. Wang, *J. Controlled Release*, 2022, **344**, 147–156.
138 L. Xu, Y. Chen, P. Zhang, J. Tang, Y. Xue, H. Luo, R. Dai, J. Jin and J. Liu, *Biomater. Sci.*, 2022, **10**, 5648–5661.
139 D. Li, J. Zhang, J. Zhang, J. Ding, H. Sun, X. Qu and J. Zhang, *ACS Appl. Polym. Mater.*, 2025, **7**, 4414–4426.
140 S. Chen, Y. Luo, Y. He, M. Li, Y. Liu, X. Zhou, J. Hou and S. Zhou, *Nat. Commun.*, 2024, **15**, 814.
141 M. Zhang, H. Qiu, Z. Han, Y. Ma, J. Hou, J. Yuan, H. Jia, M. Zhou, H. Lu and Y. Wu, *Int. J. Pharm.: X*, 2025, **9**, 100316.
142 A. Barra, J. K. Wychowaniec, D. Winning, M. M. Cruz, L. P. Ferreira, B. J. Rodriguez, H. Oliveira, E. Ruiz-Hitzky, C. Nunes and D. F. Brougham, *Adv. Healthcare Mater.*, 2024, **13**, 2303861.
143 M. S. Yoon, J. M. Lee, M. J. Jo, S. J. Kang, M. K. Yoo, S. Y. Park, S. Bong, C.-S. Park, C.-W. Park and J.-S. Kim, *Gels*, 2025, **11**, 520.
144 L. Dinh, S.-J. Hwang and B. Yan, *Pharmaceutics*, 2025, **17**, 897.
145 J. Kim, P. A. Archer, M. P. Manspeaker, A. R. Avecilla, B. P. Pollack and S. N. Thomas, *J. Controlled Release*, 2023, **357**, 655–668.
146 P. Theodosis-Nobelos, D. Charalambous, C. Triantis and M. Rikkou-Kalourkoti, *Curr. Drug Delivery*, 2020, **17**, 542–557.
147 R. Emadi, Z. Amiri, F. M. Moghadam, S. Raoufi, M. Z. Moradi, S. Asadi, W. C. Cho, J. H. Park, A. Voosough and M. R. Farani, *RSC Adv.*, 2026, **16**, 5088–5127.
148 H. Chen, Z. Wang, Y. Huang, A. Li, X. Xiong, Y. Pu and L. Guo, *Theranostics*, 2026, **16**, 580.
149 M. Nambiar and J. P. Schneider, *J. Pept. Sci.*, 2022, **28**, e3377.
150 H. Su, Y. Zhang, L. Li, X. Jiang, H. Liu, X. Guo, X. Huang, L. Zhou, C. Liu and X.-C. Shen, *Eur. Polym. J.*, 2024, **214**, 113158.
151 N. Ding, K. He, H. Tian, L. Li, Q. Li, S. Lu, K. Ding, J. Liu, E. C. Nice and W. Zhang, *Mater. Today Bio*, 2023, **20**, 100645.
152 Y. Lee, M. Kim, N. Kim, S. Byun, S. Seo and J. Y. Han, *Appl. Sci.*, 2025, **15**, 11599.
153 C. Mo, R. Luo and Y. Chen, *Macromol. Rapid Commun.*, 2022, **43**, 2200007.
154 R. W. Korsmeyer, *Polym. Controlled Drug Delivery*, 2023, 15–37.
155 S. Pardeshi, F. Damiri, M. Zehravi, R. Joshi, H. Kapare, M. K. Prajapati, N. Munot, M. Berrada, P. S. Giram and S. Rojekar, *Polymers*, 2022, **14**, 3126.
156 S. H. Pham, Y. Choi and J. Choi, *Pharmaceutics*, 2020, **12**, 630.
157 S. Adepu and S. Ramakrishna, *Molecules*, 2021, **26**, 5905.
158 F. M. Kashkooli, M. Soltani and M. Souri, *J. Contr. Release*, 2020, **327**, 316–349.
159 G. Chakrapani, M. Zare and S. Ramakrishna, *Mater. Adv.*, 2022, **3**, 7757–7772.
160 S. Wang, W. Y. Wu, J. C. C. Yeo, X. Y. D. Soo, W. Thitsartarn, S. Liu, B. H. Tan, A. Suwardi, Z. Li and Q. Zhu, *BMEMat*, 2023, **1**, e12021.
161 X. Li and X. Su, *J. Mater. Chem. B*, 2018, **6**, 4714–4730.
162 J. Gu, G. Zhao, J. Yu, P. Xu, J. Yan, Z. Jin, S. Chen, Y. Wang, L. W. Zhang and Y. Wang, *J. Nanobiotechnol.*, 2022, **20**, 372.
163 T. Nie, Y. Fang, R. Zhang, Y. Cai, X. Wang, Y. Jiao and J. Wu, *Bioact. Mater.*, 2025, **47**, 51–63.
164 C. R. Madhu and B. H. Patel, *Curr. Phys. Chem.*, 2024, **14**, 93–115.
165 J. Singh and P. Nayak, *J. Polym. Sci.*, 2023, **61**, 2828–2850.
166 Y. Yu, L. Zhang, B. Hu, Z. Wang, Q. Gu, W. Wang, C. Zhu and S. Wang, *Carbohydr. Polym.*, 2024, **339**, 122262.
167 X. Lin, H. Long, Z. Zhong, Q. Ye and B. Duan, *Int. J. Biol. Macromol.*, 2024, **270**, 132187.
168 Y. Huang, H. Lai, J. Jiang, X. Xu, Z. Zeng, L. Ren, Q. Liu, M. Chen, T. Zhang and X. Ding, *Asian J. Pharm. Sci.*, 2022, **17**, 679–696.
169 L. Luo, Y. Qi, H. Zhong, S. Jiang, H. Zhang, H. Cai, Y. Wu, Z. Gu, Q. Gong and K. Luo, *Acta Pharm. Sin. B*, 2022, **12**, 424–436.
170 D. Lin, J. Piao, Y. Wang, Y. Chen, S. Shi, J. Cao, H. Shi and Q. Zhang, *Compos. Commun.*, 2024, **47**, 101882.
171 N. R. Boase, E. R. Gillies, R. Goh, R. E. Kieltyka, J. B. Matson, F. Meng, A. Sanyal and O. Sedlacek, *Biomacromolecules*, 2024, **25**, 5417–5436.
172 H. F. Abed, W. H. Abuwatfa and G. A. Husseini, *Nanomaterials*, 2022, **12**, 3183.
173 X. Ding, M. Zang, Y. Zhang, Y. Chen, J. Du, A. Yan, J. Gu, Y. Li, S. Wei and J. Xu, *Acta Biomater.*, 2023, **167**, 182–194.
174 T. T. Vu, M. Gulfam, S.-H. Jo, S.-H. Park and K. T. Lim, *Carbohydr. Polym.*, 2022, **278**, 118964.
175 L. Mei, Q. Mei, W. Dong and S. Wu, *Appl. Mater. Today*, 2024, **41**, 102471.

176 X. An, W. Yu, J. Liu, D. Tang, L. Yang and X. Chen, *Cell Death Dis.*, 2024, **15**, 556.
177 M. Criado-Gonzalez and D. Mecerreyes, *J. Mater. Chem. B*, 2022, **10**, 7206–7221.
178 M. Pu, H. Cao, H. Zhang, T. Wang, Y. Li, S. Xiao and Z. Gu, *Mater. Horiz.*, 2024, **11**, 3721–3746.
179 H. Ruan, Q. Hu, D. Wen, Q. Chen, G. Chen, Y. Lu, J. Wang, H. Cheng, W. Lu and Z. Gu, *Adv. Mater.*, 2019, **31**, 1806957.
180 N. Gao, Y. Huang, S. Jing, M. Zhang, E. Liu, L. Qiu, J. Huang, B. Muhitdinov and Y. Huang, *Theranostics*, 2024, **14**, 3810.
181 A. Goenka, F. Khan, B. Verma, P. Sinha, C. C. Dmello, M. P. Jogalekar, P. Gangadaran and B. C. Ahn, *Cancer Commun.*, 2023, **43**, 525–561.
182 X. Jing, H. Hu, Y. Sun, B. Yu, H. Cong and Y. Shen, *Small Methods*, 2022, **6**, 2101437.
183 M. Shahriari, M. Zahiri, K. Abnous, S. M. Taghdisi, M. Ramezani and M. Alibolandi, *J. Controlled Release*, 2019, **308**, 172–189.
184 S. Zhao, N. Yu, H. Han, S. Guo and N. Murthy, *Curr. Opin. Chem. Biol.*, 2025, **84**, 102552.
185 G. Lin, X. Li, G. Nowaczyk and W. Wang, *Chem Bio Eng.*, 2025, **2**, 283–302.
186 J. Omar, D. Ponsford, C. A. Dreiss, T. C. Lee and X. J. Loh, *Chem.–Asian J.*, 2022, **17**, e202200081.
187 J. Chen, J. Ma, Z. Xu, H. Luo and C. Qian, *Front. Pharmacol*, 2025, **16**, 1627883.
188 Z. Chen, H. Wu, Y. Wang, Y. Rao, J. Yan, B. Ran, Q. Zeng, X. Yang, J. Gao and H. Gao, *Acta Biomater.*, 2024, **188**, 79–92.
189 W. Jia, R. Liu, Y. Wang, C. Hu, W. Yu, Y. Zhou, L. Wang, M. Zhang, H. Gao and X. Gao, *Acta Pharm. Sin. B*, 2022, **12**, 3354–3366.
190 C. Wu, C. Wang, Y. Zheng, Y. Zheng, Z. Liu, K. Xu and W. Zhong, *Adv. Funct. Mater.*, 2021, **31**, 2104418.
191 Z. Chen, Y. Rong, J. Ding, X. Cheng, X. Chen and C. He, *Pharmaceutics*, 2023, **15**, 428.
192 J. Liu, T. Yang, L. Dai, K. Shi, Y. Hao, B. Chu, D. Hu, Z. Bei, L. Yuan and M. Pan, *Bioact. Mater.*, 2024, **31**, 315–332.
193 Q. Luo, J. Sun, Z. Li, B. Liu and J. Ding, *Chin. Chem. Lett.*, 2024, 110433.
194 R. Fan, Y. Cheng, R. Wang, T. Zhang, H. Zhang, J. Li, S. Song and A. Zheng, *Polymers*, 2022, **14**, 2379.
195 Y. Gong, W. Yuan, S. Liu, M. Jin, S. Li, L. Tao, Y. Chu, H. Li, Y. Yu and X. Chen, *Adv. Healthcare Mater.*, 2025, 2500511.
196 Y. Li, J. Zhu, Y. Yang, Y. Chen, L. Liu, J. Tao, H. Chen and Y. Deng, *Mol. Pharm.*, 2023, **20**, 6345–6357.
197 K. C. Kloepping, A. S. Kraus, D. K. Hedlund, C. M. Gnade, B. A. Wagner, M. L. McCormick, M. A. Fath, D. Seol, T.-H. Lim and G. R. Buettner, *PLoS One*, 2020, **15**, e0244540.
198 X. Liu, Y. Zhang, Y. Wang, W. Zhu, G. Li, X. Ma, Y. Zhang, S. Chen, S. Tiwari and K. Shi, *Theranostics*, 2020, **10**, 3793.
199 B. Govindan, M. A. Sabri, A. Hai, F. Banat and M. A. Haija, *Pharmaceutics*, 2023, **15**, 868.
200 S. Ganguly and S. Margel, *Polymers*, 2021, **13**, 4259.
201 Z. Li, X. Liang, Z. Qiu, Z. Liu, S. Wang, Y. Zhou and N. Li, *Chin. Chem. Lett.*, 2024, **35**, 109592.
202 A. Kasiński, A. Świerczek, M. Zielińska-Pisklak, S. Kowalczyk, A. Plichta, A. Zgadzaj, E. Oledzka and M. Sobczak, *Int. J. Mol. Sci.*, 2023, **24**, 6906.
203 Y. Xing, B. Zeng and W. Yang, *Front. Bioeng. Biotechnol.*, 2022, **10**, 1075670.
204 P. Zhang, G. Wang and H. Yu, *Responsive Mater.*, 2024, **2**, e20240016.
205 X. Liu, M. Shen, T. Bing, X. Zhang, Y. Li, Q. Cai, X. Yang and Y. Yu, *Adv. Sci.*, 2024, **11**, 2402208.
206 L. Chang, X. Liu, J. Zhu, Y. Rao, D. Chen, Y. Wang, Y. Zhao and J. Qin, *Colloids Surf., B*, 2022, **218**, 112747.
207 W. Zhou, S. Lei, M. Liu, D. Li, Y. Huang, X. Hu, J. Yang, J. Li, M. Fu and M. Zhang, *Biomaterials*, 2022, **291**, 121872.
208 H. Hyun, M. H. Park, G. Jo, B. Y. Lee, J. W. Choi, H. J. Chun, H. S. Kim and D. H. Yang, *Nanomaterials*, 2021, **11**, 317.
209 S. Joseph, R. Chakrabarty and P. Paira, *Dalton Trans.*, 2025, **54**, 13820–13850.
210 J. P. Pham, A. M. Joshua, I. P. da Silva, R. Dummer and S. M. Goldinger, *Curr. Oncol. Rep.*, 2023, **25**, 609–621.
211 R. Mathiyalagan, M. Murugesan, Z. M. Ramadhania, J. Nahar, P. Manivasagan, V. Boopathi, E.-S. Jang, D. C. Yang, J. Conde and T. Thambi, *Mater. Sci. Eng. R Rep.*, 2024, **160**, 100824.
212 D. Miao, R. Luo, Y. Li, X. Qin, Y. Wang, Y. Zhang, T. Yi, H. Wang, B. Zheng and R. Huang, *Adv. Mater.*, 2025, 2502455.
213 J. Li, G. Luo, C. Zhang, S. Long, L. Guo, G. Yang, F. Wang, L. Zhang, L. Shi and Y. Fu, *Mater. Today Bio*, 2022, **14**, 100238.
214 R. Sun, Y. Chen, Q. Yang, W. Zhang, L. Guo and M. Feng, *Int. J. Pharm.*, 2022, **613**, 121390.
215 V. Borzillo and P. Muto, *Cancers*, 2021, **13**, 5859.
216 J. B. Shimol, Y. Guzman-Prado, M. Karlinskaya and T. Davidson, *Crit. Rev. Oncol. Hematol.*, 2021, **167**, 103499.
217 M. Zhu, L. Zhao and X. Lu, *Int. J. Nanomed.*, 2024, 11805–11818.
218 J. Zhang, L. Yang, F. Huang, C. Zhao, J. Liu, Y. Zhang and J. Liu, *Adv. Healthcare Mater.*, 2021, **10**, 2101190.
219 Y. C. Dong, L. M. Nieves, J. C. Hsu, A. Kumar, M. Bouché, U. Krishnan, K. J. Mossburg, D. Saxena, S. Uman and T. Kambayashi, *Chem. Mater.*, 2023, **35**, 9542–9551.
220 Z. Cui, L. Wang, W. Liu, D. Xu, T. Zhang, B. Ma, K. Zhang, L. Yuan, Z. Bing and J. Liu, *Adv. Healthcare Mater.*, 2024, **13**, 2401438.
221 M. Overchuk, R. A. Weersink, B. C. Wilson and G. Zheng, *ACS Nano*, 2023, **17**, 7979–8003.
222 A. Campu, M. Focsan, F. Lerouge, R. Borlan, L. Tie, D. Rugina and S. Astilean, *Colloids Surf., B*, 2020, **194**, 111213.
223 G. Gao, X. Sun and G. Liang, *Adv. Funct. Mater.*, 2021, **31**, 2100738.
224 R. L. Ge, P. N. Yan, Y. Liu, Z. S. Li, S. Q. Shen and Y. Yu, *Adv. Funct. Mater.*, 2023, **33**, 2301138.
225 X. Zhao, J. Liu, J. Fan, H. Chao and X. Peng, *Chem. Soc. Rev.*, 2021, **50**, 4185–4219.
226 W. Jiang, M. Liang, Q. Lei, G. Li and S. Wu, *Cancers*, 2023, **15**, 585.

227 D. An, J. Fu, B. Zhang, N. Xie, G. Nie, H. Ågren, M. Qiu and H. Zhang, *Adv. Funct. Mater.*, 2021, **31**, 2101625.
228 X. Huang, L. Tang, L. Xu, Y. Zhang, G. Li, W. Peng, X. Guo, L. Zhou, C. Liu and X.-C. Shen, *J. Mater. Chem. B*, 2022, **10**, 7717–7731.
229 X. Tang, X. Chen, S. Zhang, X. Gu, R. Wu, T. Huang, Z. Zhou, C. Sun, J. Ling and M. Liu, *Adv. Funct. Mater.*, 2021, **31**, 2101320.
230 Y. Chi, Y. Zheng, X. Pan, Y. Huang, Y. Kang, W. Zhong and K. Xu, *Acta Biomater.*, 2024, **174**, 127–140.
231 T. Chen, T. Yao, H. Peng, A. K. Whittaker, Y. Li, S. Zhu and Z. Wang, *Adv. Funct. Mater.*, 2021, **31**, 2106079.
232 V. Mohammadzadeh, H. Atapour-Mashhad, S. Shahvali, B. Salehi, M. Shaban, M. Shirzad, A. Salahvarzi and M. Mohammadi, *J. Nanobiotechnol.*, 2025, **23**, 545.
233 H. S. Seo, C.-P. J. Wang, W. Park and C. G. Park, *Tissue Eng. Regener. Med.*, 2022, **19**, 263–280.
234 N. Shajari, B. Baradaran, M. R. Tohidkia, H. Nasiri, M. Sepehri, S. Setayesh and L. Aghebati-Maleki, *Curr. Treat. Options Oncol.*, 2024, **25**, 1073–1088.
235 H. Liu, X. Gou, Y. Tan, Q. Fan and J. Chen, *Hum. Vaccines Immunother.*, 2024, **20**, 2394252.
236 L. Tagliaferri, V. Lancellotta, B. Fionda, M. Mangoni, C. Casà, A. Di Stefani, M. M. Pagliara, A. D'Aviero, G. Schinzari and S. Chiesa, *Hum. Vaccines Immunother.*, 2022, **18**, 1903827.
237 Y. Wang, C. Jiang, H. Zhou and R. Han, *Exp. Hematol. Oncol.*, 2025, **14**, 114.
238 J. Kim, D. M. Francis, L. F. Sestito, P. A. Archer, M. P. Manspeaker, M. J. O'Melia and S. N. Thomas, *Nat. Commun.*, 2022, **13**, 1479.
239 S. N. Lucas, P. A. Archer, T. H. Yoon, M. P. Manspeaker, M. Levitan, J. Kim and S. N. Thomas, *ACS Nano*, 2025, **19**, 21775–21791.
240 Y. Yang, B. Zhang, Y. Xu, W. Zhu, Z. Zhu, X. Zhang, W. Wu, J. Chen and Z. Yu, *Bioact. Mater.*, 2024, **42**, 178–193.
241 H. Zhu, X. Peng, Y. Liu, X. Zhang, X. Zhang, T. Li, H. Liu, S. Yang, J. Zhang and B. He, *Adv. Funct. Mater.*, 2025, 2420553.
242 D. Sun, X. Sun, X. Zhang, J. Wu, X. Shi, J. Sun, C. Luo, Z. He and S. Zhang, *Adv. Healthcare Mater.*, 2024, **13**, 2400809.
243 P. Zhao, H. Li and W. Bu, *Angew. Chem., Int. Ed.*, 2023, **62**, e202210415.
244 Y. Zhou, S. Fan, L. Feng, X. Huang and X. Chen, *Adv. Mater.*, 2021, **33**, 2104223.
245 S. Li, B. Wang, J. Tao, Y. Dong, T. Wang, X. Zhao, T. Jiang, L. Zhang and H. Yang, *Int. J. Pharm.*, 2024, **660**, 124330.
246 Y. Zhang, X. Zhang, L. Zhang, J. Yao, S. Wang, J. Zhao, H. Sun and Z. Li, *Colloids Surf., A*, 2024, **690**, 133748.
247 M. Chen, Y. Liu, Y. Tang, Z. Li, R. Yang, Y. Wei, Z. Liang, W. Han, L. Zhao and D. Huang, *Colloids Surf., A*, 2025, 138760.
248 W. Pi, L. Wu, J. Lu, X. Lin, X. Huang, Z. Wang, Z. Yuan, H. Qiu, J. Zhang and H. Lei, *Bioact. Mater.*, 2023, **29**, 98–115.
249 X. Zhang, J. Huang, J. Huang, Z. Shi, H. Niu, Y. Zheng, X. Wang, C. Wu, J. Chen and P. Liu, *Adv. Funct. Mater.*, 2025, **35**, 2417871.
250 J. R. Clegg, K. Adebowale, Z. Zhao and S. Mitragotri, *Bioeng. Transl. Med.*, 2024, **9**, e10680.
251 S. Aswathy, U. Narendrakumar and I. Manjubala, *Heliyon*, 2020, **6**, e03719.
252 K. Xue, X. Wang, P. W. Yong, D. J. Young, Y. L. Wu, Z. Li and X. J. Loh, *Adv. Therapeut.*, 2019, **2**, 1800088.